



# HHS Public Access

Author manuscript

*Adv Healthc Mater.* Author manuscript; available in PMC 2022 June 01.

Published in final edited form as:

*Adv Healthc Mater.* 2021 June ; 10(11): e2001986. doi:10.1002/adhm.202001986.

## Multi-dimensional Printing for Bone Tissue Engineering

**Moyuan Qu,**

Department of Bioengineering, California NanoSystems Institute and Center for Minimally Invasive Therapeutics (C-MIT) University of California, Los Angeles, Los Angeles, CA 90095, USA

The Affiliated Hospital of Stomatology, School of Stomatology, Zhejiang University School of Medicine and Key Laboratory of Oral Biomedical Research of Zhejiang Province, Hangzhou, Zhejiang, 310006, China

**Canran Wang,**

Department of Bioengineering, California NanoSystems Institute and Center for Minimally Invasive Therapeutics (C-MIT) University of California, Los Angeles, Los Angeles, CA 90095, USA

**Xingwu Zhou,**

Department of Bioengineering, California NanoSystems Institute and Center for Minimally Invasive Therapeutics (C-MIT) University of California, Los Angeles, Los Angeles, CA 90095, USA

Department of Chemical and Biomolecular Engineering, University of California-Los Angeles, Los Angeles, CA 90095, USA

**Alberto Libanori,**

Department of Bioengineering, California NanoSystems Institute and Center for Minimally Invasive Therapeutics (C-MIT) University of California, Los Angeles, Los Angeles, CA 90095, USA

**Xing Jiang,**

Department of Bioengineering, California NanoSystems Institute and Center for Minimally Invasive Therapeutics (C-MIT) University of California, Los Angeles, Los Angeles, CA 90095, USA

School of Nursing, Nanjing University of Chinese Medicine, Nanjing 210023, China

**Weizhe Xu,**

The Affiliated Hospital of Stomatology, School of Stomatology, Zhejiang University School of Medicine and Key Laboratory of Oral Biomedical Research of Zhejiang Province, Hangzhou, Zhejiang, 310006, China

**Songsong Zhu,**

---

\* khademh@terasaki.org; wsun@terasaki.org.

Conflict of Interest

The authors declare no conflict of interest.

State Key Laboratory of Oral Diseases, National Clinical Research Center for Oral Diseases, West China Hospital of Stomatology, Sichuan University, Chengdu 610041, China

**Qianming Chen,**

The Affiliated Hospital of Stomatology, School of Stomatology, Zhejiang University School of Medicine and Key Laboratory of Oral Biomedical Research of Zhejiang Province, Hangzhou, Zhejiang, 310006, China

**Wujin Sun\***,

Department of Bioengineering, California NanoSystems Institute and Center for Minimally Invasive Therapeutics (C-MIT) University of California, Los Angeles, Los Angeles, CA 90095, USA

Terasaki Institute for Biomedical Innovation, Los Angeles, California 90064, United States

**Ali Khademhosseini\***

Department of Bioengineering, California NanoSystems Institute and Center for Minimally Invasive Therapeutics (C-MIT) University of California, Los Angeles, Los Angeles, CA 90095, USA

Department of Chemical and Biomolecular Engineering, University of California-Los Angeles, Los Angeles, CA 90095, USA

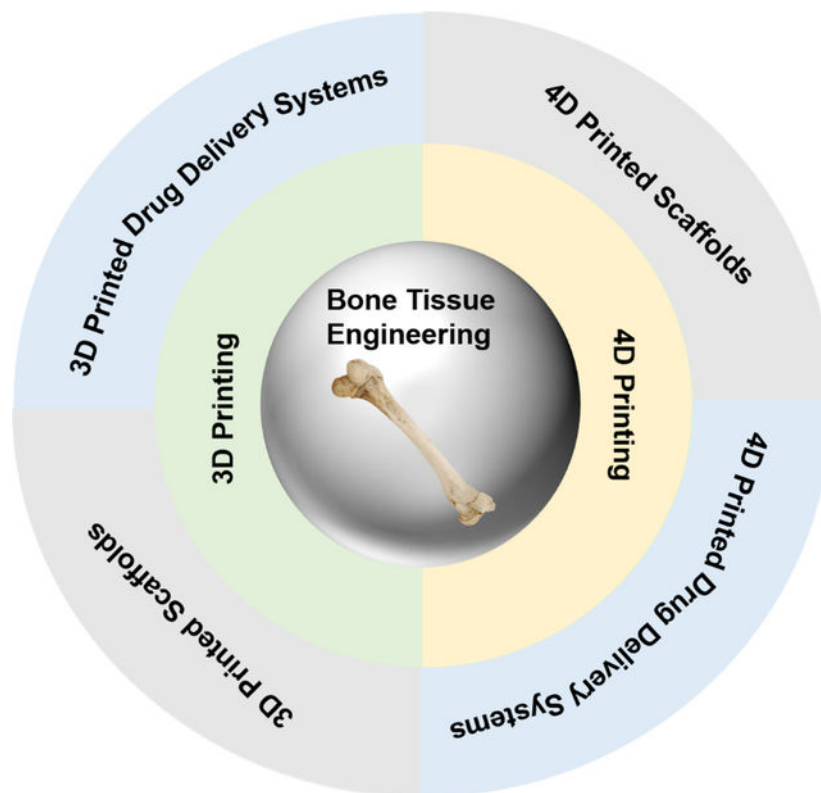
Jonsson Comprehensive Cancer Center, Department of Radiology University of California-Los Angeles, Los Angeles, CA 90095, USA

Terasaki Institute for Biomedical Innovation, Los Angeles, California 90064, United States

## Abstract

The development of three-dimensional (3D) printing has significantly advanced the field of bone tissue engineering by enabling the fabrication of scaffolds that faithfully recapitulate desired mechanical properties and architectures. In addition, computer-based manufacturing relying on patient-derived medical images permits the fabrication of customized modules in a patient-specific manner. In addition to conventional 3D fabrication, progress in materials engineering has led to the development of four-dimensional (4D) printing, allowing time-sensitive interventions such as programed therapeutics delivery and modifiable mechanical features. Therapeutic interventions established *via* multi-dimensional engineering are expected to enhance the development of personalized treatment in various fields, including bone tissue regeneration. Here, we summarized recent studies utilizing 3D printed systems for bone tissue regeneration and highlight advances in 4D printed systems. We also discussed challenges and perspectives for the future development of multi-dimensional printed systems towards personalized bone regeneration.

## Graphical Abstract



## Keywords

3D printing; 4D printing; drug delivery; bone; tissue engineering; additive manufacturing; three-dimensional (3D) printing; scaffold

## 1. Introduction

In spite of bones' remarkable self-healing capabilities, healing of large-scale bone defects remains challenging, especially when medical intervention is absent.<sup>[1, 2]</sup> In the clinic, the gold standard treatments to address such large-scale bone defects include the filling of defects with autologous bone parts or allografts. However, donor site morbidity and finite bone supply largely limit the efficacy of such treatments.<sup>[3]</sup> Tissue engineering represents a promising alternative to replacing defected or diseased tissues, allowing the recovery of the affected bones through engineering materials, cells, and growth factors (GFs).<sup>[4, 5]</sup>

Scaffolds fabricated as porous three dimensional (3D) biocompatible structures play an essential role in bone tissue engineering, as they provide mechanical support for cell seeding and a template for neo-tissue regeneration.<sup>[6]</sup> In addition, biochemical regenerative cues such as protein-based biomolecules (e.g., GFs) can also be incorporated.<sup>[7]</sup> In this regard, scaffolds with desirable physical features and biomolecule delivery capabilities would be ideal candidates to enhance bone healing.

Natural bone tissue is comprised of two distinct types of structures: cancellous bone (with 50% - 90% porosity) and cortical bone (with < 10% porosity).<sup>[1]</sup> Traditional methods, including phase separation, foaming, or particulate leaching, have been used to fabricate porous scaffolds<sup>[8]</sup>, but customizing desired porosity gradients that mimic natural bones remains a challenge. Bone defects often involve the injury of surrounding cartilage and soft tissues in clinic. The regeneration of bone also needs the formation of nerve and vascular tissues. However, it is still a challenge to fabricate scaffolds integrated with multiple types of cells for osteochondral or vascularized bone regeneration. 3D printing technologies are promising to advance the field of personalized and integrated bone tissue engineering.<sup>[1, 3, 9, 10]</sup> 3D printing, also known as additive manufacturing, allows the fabrication of complex structures using layer-by-layer deposition of materials.<sup>[11]</sup> For bone tissue engineering, multiple additive manufacturing techniques have been utilized, including direct extrusion, stereolithography, fused deposition, and selective laser sintering.<sup>[3, 12]</sup> These techniques allow the production of customized shapes based on medical images. They also enable the control of physical properties, such as the distribution of porosity, to mimic the structures of cancellous and cortical bones. In addition, by utilizing 3D bioprinted constructs with multiple cell types and biocompatible matrices, post-implantation bone formation can be facilitated by encapsulating cells and bioactive molecules within the matrices.<sup>[13]</sup>

Besides engineering tissue scaffolds, 3D printing has been applied for drug delivery.<sup>[14, 15]</sup> In August 2015, the first FDA-approved 3D-printed drug formulation (Spritam<sup>®</sup>(levetiracetam)) demonstrated the feasibility of applying 3D printing in drug delivery.<sup>[15, 16]</sup> Spritam<sup>®</sup> is a fast dissolving tablet formulation fabricated based on powder bed-liquid 3D printing technology (ZipDose<sup>®</sup>) for the treatment of seizures.<sup>[17]</sup> The approval of Spritam<sup>®</sup> indicates that it is promising to fabricate personalized drug delivery systems (DDS) with multiple components to achieve spatially and temporally programable drug delivery, which can enhance therapeutic effects and reduce adverse reactions.<sup>[15]</sup> In the early stage of bone regeneration, neovascularization is necessary for the transportation of stem cells, nutrition, and oxygen.<sup>[18]</sup> Co-delivery of osteogenic and angiogenic growth factors has been demonstrated as an effective strategy for bone regeneration.<sup>[19]</sup> Compared with simultaneous release of both factors, delayed release of osteogenic growth factors mimicked the natural angiogenic-osteogenic process and led to better bone formation.<sup>[20]</sup> In this context, 3D printed systems are very promising in delivering personalized and programmed drug-releasing scaffolds for bone regeneration. With customizable 3D structures and programmable drug release profiles, these engineered scaffolds can significantly enhance bone healing efficacy.<sup>[21]</sup>

To further simulate the dynamic *in vivo* environment, four-dimensional (4D) printing approaches enable the incorporation of ‘time’ into current 3D printing by the use of smart materials.<sup>[22, 23]</sup> Both shape-changing and programmable drug release capabilities of 4D-printed structures can benefit bone tissue engineering. For instance, considering the bone defects comes with different shapes, scaffolds printed with shape-memory materials can be reshaped and implanted in a minimally invasive manner. The scaffolds’ shape recovery that followed can make them fit the irregular bone defects precisely.<sup>[1, 24]</sup>

In this review, we summarized recent progress in 3D printed scaffolds, 3D printed DDS and 4D printing for enhanced bone tissue regeneration (Figure 1). In addition, challenges and opportunities for the future development of multi-dimensional printed medical devices for bone regeneration are also discussed.

## 2. 3D printed scaffolds for bone regeneration.

3D printing methods enable accurate control of scaffold microstructures as well as compositions at the microscale, making them powerful tools in the fabrication of medical devices.<sup>[25]</sup> A patient-specific bone-graft substitute can be fabricated with a Computer-Aided Design (CAD) file and a 3D printer. CAD models based on patients' X-ray computed tomography (X-ray CT) or magnetic resonance imaging (MRI) enable such a personalized approach.<sup>[26]</sup> The commonly used 3D printing techniques for bone tissue engineering include 3D plotting/direct ink writing, stereolithography (SLA), selective laser sintering (SLS), selective laser melting (SLM), fused deposition modeling (FDM), and inkjet/extrusion-based bioprinting.<sup>[1, 27]</sup> Because of the various mechanisms of different 3D printing techniques, understanding the impact of different printing materials, and evaluating the advantages or disadvantages of each 3D printing process, can guide designers to choose an optimal 3D printing technique for bone engineering. Table 1 summarizes the representative 3D printing techniques employed for bone regeneration applications, including known advantages and drawbacks. Moreover, recent progress in 3D printed scaffolds for bone tissue engineering is also summarized in terms of the materials (Table 2).

### 2.1 Organic scaffolds

**2.1.1. Polymer-based scaffolds**—Polymers have been widely used for bone regeneration.<sup>[73]</sup> With proper modifications, polymer-based systems can achieve high biocompatibility and efficiency in bone regeneration. For example, Kwon and colleagues printed poly( $\epsilon$ -caprolactone) (PCL)-blended polyethylene glycol (PEG) to engineer scaffolds. The hydrophilicity of PEG enabled the formation of porous structures, which facilitated cell proliferation. The scaffold was shown to enhance the survival of the osteosarcoma-derived cell line, MG 63 cells. Higher cell density with increased protein secretion was observed in PCL/PEG scaffolds, which demonstrated the effectiveness of the polymer-based system for osteogenesis.<sup>[66]</sup>

Conductive polymers have also been widely applied for bone regeneration since electric signals are known as positive contributors to osteogenesis.<sup>[97]</sup> Electric signals, which stimulate cell signaling, can be propagated by conductive composites. Biocompatible conductive polymers, including polyaniline (PANI), polypyrrole (PPy), and poly(3,4-ethylenedioxythiophene) (PEDOT), provided new approaches for bone tissue engineering.<sup>[98]</sup> Bartolo et al. embedded PANI microparticles inside PCL polymers to enhance the electric conductivity of a printed matrix. The addition of PANI also improved the mechanical suitability of the scaffolds for bone regeneration. However, if compared with natural hydrogel, PANI has slight cytotoxicity, which limited its concentration in the 3D-printed scaffolds. In the group with 0.1%, 1%, and 2% (w/w) PANI loaded in PCL, human adipose-derived stem cells (hADSCs) exhibited promoted proliferation.<sup>[67]</sup> PEDOT, known

for its processability and biocompatibility among conductive polymers, has also been used in bone tissue engineering.<sup>[99]</sup> For example, Simon and co-workers printed PCL scaffolds with a PEDOT coating. They employed vapor-phase polymerization (VPP) to coat PEDOT on PCL and added tosylate for polymerization, generating the final product PEDOT:Tos. In order to form a continuous PEDOT:Tos coating, polyridine (Pyr) or PEG-PPG-PEG (PPP) were added to tune the polymerization process during VPP. To validate the scaffolds in bone engineering, the authors directly cultured mesenchymal stem cells (MSCs) on the PCL scaffolds with or without PEDOT coating. Good cytocompatibility of both Pyr-PEDOT:Tos and PPP-PEDOT:Tos-coated PCL scaffolds for MSCs was shown, suggesting their potential use in osteogenesis.<sup>[68]</sup> Other researchers have reported the use of ice templates to form porous poly(3,4-ethylenedioxythiophene):poly(styrenesulfonate) (PEDOT:PSS) scaffolds to improve osteogenesis, further advancing polymer-based systems in bone engineering.<sup>[69]</sup> Furthermore, researchers have incorporated PEDOT:PSS with gelatin methacryloyl (GelMA) to improve printability and biocompatibility of the conductive material.<sup>[70]</sup> With advances in material optimization, polymer-based conductive systems will contribute more to bone engineering.

Hydrogels, which are crosslinked 3D polymeric networks, have also captured a lot of attention for bone tissue engineering.<sup>[100]</sup> They can generate porous structures for entrapping cells or proteins.<sup>[101]</sup> Swellable in an aqueous microenvironment, the crosslinked networks of hydrogel have high water contents and tissue-like elastic properties. High water content of hydrogels contributes to the incorporation of cells for bone regeneration.<sup>[102]</sup> However, low mechanical strength of hydrogels is a major concern in bone regeneration applications. To address this challenge, Kim et al. used silk fibroin (SF), a natural material with enhanced strength, as the main component of the hydrogel matrix. The authors also employed the decellularized extracellular matrix (dECM) extracted from preosteoblast cells (MC3T3-E1). The mixture of dECM and collagen provided bioactive signals to guide cell differentiation and maintained certain degrees of viscosity for 3D printing. Compared with pure collagen scaffolds, 3D printed collagen/dECM/SF scaffolds promoted the osteogenic activity of pre-osteoblast cells by inducing the expression of alkaline phosphatase (ALP), an early-stage osteogenesis marker, as well as deposition of calcium ions. Accelerated cell proliferation was observed in the matrix containing dECM, collagen, and silk, compared to those embedded in pure collagen or collagen with dECM.<sup>[65]</sup>

3D printing of tough hydrogels is another emerging technique used in bone tissue engineering. Hydrogels with high strength have been used for bone regeneration, and various printable tough hydrogels have been developed with high fracture toughness to withstand physiological mechanical loads.<sup>[103]</sup> For instance, Cui et al. synthesized a tough polyion complex (PIC) hydrogels for 3D printing. Specifically, the authors used direct sol-gel transition, an innovative fabrication mechanism to develop a tough hydrogel suitable for extrusion-based printing. Within the PIC hydrogel, multiwalled carbon nanotubes (MWCNTs) were incorporated to help with the osteogenesis and calcification processes. In this study, the researchers leveraged the advantages of 3D printing to form a porous PIC/MWCNT nanocomposite scaffold. Such scaffolds were validated to facilitate the osteogenic differentiation of rat bone marrow MSCs. After implantation in rats, similar results were shown for the PIC/MWCNT scaffold, including accelerated bone defect repair and

upregulated angiogenesis at the bone healing site.<sup>[104]</sup> In summary, these biocompatible hydrogel-based systems with modified printability and mechanical features showed great potential in stem cell delivery for bone regeneration.

**2.1.2. bioprinting**—With the development of solvent-free printing techniques and biocompatible inks, it is now feasible to directly print biomaterials that contain living cells.<sup>[105]</sup> By incorporating biomimic components and recapitulating mechanical properties of bone, bioprinted scaffolds can restore the functions of defected bone tissues.<sup>[106]</sup> Fischer and co-workers bioprinted collagen-based hydrogels that encapsulated MSCs. Collagen is naturally found within bones and is a known trigger for osteogenesis. The addition of agarose into collagen contributed to the implant's mechanical strength, promoting MSCs differentiation for bone regeneration. However, the poor printability of agarose limited its percentage in the hydrogel matrix. By optimizing the ratio of collagen and agarose, 3D-printable hydrogels, termed AGx-COLy have been developed, which showed high printing resolutions. *In vitro* studies confirmed better spread and elongation of cells embedded in AGx-COLy than those in agarose only. Overall, the as-prepared matrix loaded with MSCs demonstrated high potential as a therapeutic delivery vehicle.<sup>[71]</sup> With different bioinks, different parameters need to be optimized to screen the optimal formulation for bone tissue engineering. For instance, Ouyang et al. utilized complementary network bioinks made from a library of polymers (including gelatin, hyaluronic acid, chondroitin sulfate, dextran, alginate, chitosan, heparin, and poly(ethylene glycol)) to screen the optimal formulation for bone tissue regeneration. The composite GelMA + gelatin bioink demonstrated the most efficient osteogenic activity and mineralization on osteogenic sarcoma cell line (Saos-2).<sup>[72]</sup> To enhance the mechanical strength of the bioprinted hydrogel scaffolds, 3D printed supporting structures with solid polymers were employed. By using a fiber engraving technique, Mikos and colleagues printed engraved PCL scaffolds with grooves on the surface, enabling the deposition of low viscosity bioink into this groove without lateral spreading. The authors subsequently printed fibroblasts-loaded GelMA hydrogel into the groove, further confirming the utility of the scaffold for hard tissue engineering.<sup>[73]</sup>

## 2.2 Inorganic Scaffolds

**2.2.1. Ceramic scaffolds**—The main constituent of bone is calcium phosphate (CaP) (up to 70%, w/w)<sup>[107]</sup>, scaffolds based on bioactive CaP ceramics, that mimic the structure, component, and mechanical strength of natural bone, have attracted increased interest. Bioactive CaP ceramic-based scaffolds have been reported to promote osteogenic induction of stem cells *in vitro* and *in vivo*.<sup>[108]</sup> Mechanical strength (particularly compressive strength) is an important parameter in osteoconduction, and it can be adjusted by tuning the micro/nanostructure or porosity of scaffolds.<sup>[109]</sup> Porosity of a scaffold alone is also an important parameter in osteoconduction. It has been demonstrated that small pore-associated hypoxic conditions could induce osteochondral formation before osteogenesis. Large pores could promote vascularization, leading directly to osteogenesis (without preceding cartilage formation).<sup>[110]</sup> Therefore, the mechanical strength and porosity of a scaffold should be customized for a specific purpose. With the development of 3D printing techniques, ceramic scaffolds mimicking the structure, porosity, and mechanical strength of natural bone can be fabricated to accelerate bone regeneration. To replicate the microstructure and cellular

components of natural bone, Zhang et al. reported an SLA-based 3D printing strategy to fabricate Haversian bone-mimicking scaffolds with Haversian canals, Volkman canals, and cancellous bone structure. The capability of delivering human bone mesenchymal stem cells (hBMSCs) and human umbilical vein endothelial cells (HUVECs) enabled the Haversian bone-mimicking scaffolds to induce osteogenesis, angiogenesis, and neurogenesis *in vitro* and promote the regeneration of blood vessels and bone *in vivo* (Figure 2).<sup>[74]</sup> Biphasic CaP (BCP)-based scaffolds, containing mixtures of hydroxyapatite (HA) and  $\beta$ -tricalcium phosphate ( $\beta$ -TCP), are efficient in stimulating bone regeneration due to the release of calcium and phosphate ions, excellent biocompatibility, and osteoconductivity. Zeng et al. 3D printed a microporous BCP scaffold for bone tissue engineering using an SLS and sintering strategy. They also explored the osteogenesis signaling with 3D printed scaffolds. The printed microporous BCP scaffolds showed efficient osteogenic induction *in vitro* with an ERK $\frac{1}{2}$  signaling-dependent process. The printed microporous BCP scaffolds significantly promoted precursor cell homing, accelerating bone regeneration *in vivo*.<sup>[75]</sup> To promote bone regeneration after surgical removal of a bone tumor, it is desirable to fabricate scaffolds with the capability of selectively killing the tumor cells and accelerating the bone regeneration. To achieve this goal, Dang and co-workers fabricated a copper coordinated tetrakis (4-carboxyphenyl) porphyrin (Cu-TCPP) metal-organic nanosheet-based  $\beta$ -TCP scaffold (Cu-TCPP-TCP) using 3D printing techniques. By incorporating Cu ions, the scaffold demonstrated improved angiogenesis and osteogenesis effects. Benefiting from the photothermal effect of Cu-TCPP nanosheets, printed Cu-TCPP-TCP scaffolds could serve as a photothermal therapy device when exposed to near-infrared (NIR) light. The Cu-TCPP-TCP scaffolds could accelerate bone and blood vessel regeneration by promoting the osteogenic and angiogenic differentiation of hBMSCs and HUVECs, respectively.<sup>[76]</sup> A new class of early transition metal carbides/nitrides/carbonitrides, termed as MXene, has demonstrated high photothermal conversion efficiency that is promising for photothermal therapy.<sup>[111]</sup> To endow bioactive glass scaffolds with photothermal capabilities, researchers 3D printed a novel bioactive glass scaffold integrating 2D Ti<sub>3</sub>C<sub>2</sub> MXene nanosheets to achieve concurrent anti-cancer photothermal therapy and accelerated bone tissue regeneration.<sup>[77]</sup> It has been proved that the delivery of nitric oxide (NO) can normalize tumor vasculature and immune microenvironment for anti-cancer therapy.<sup>[112]</sup> In the meantime, NO plays a key role in bone formation.<sup>[113]</sup> To enhance the anti-tumor efficacy and promote bone regeneration, Yang et al. fabricated a multifunctional system by integrating S-nitrosothiol (R-SNO)-grafted mesoporous silica and 2D Nb<sub>2</sub>C MXene nanosheets within 3D-printing bioactive glass scaffolds. After exposure to NIR, this 3D printed systems could kill Saos-2 cells (human osteosarcoma cells) by NIR-triggered hyperthermia and release of nitric oxide (NO). Moreover, the tunable NO generation and bioactive glass scaffolds could accelerate vascularization and bone regeneration.<sup>[78]</sup> Due to the recent progress in 3D printing techniques and material engineering, it is now feasible to 3D print scaffolds with biomimicking microstructures in high resolution, showing great prospects for translational applications.

**2.2.2. Metallic scaffolds**—Given the critical requirement of mechanical strength for bone substitutes, scaffolds consisting of metallic materials were commonly used in the clinic to meet the mechanical requirement and serve as functional substitutes for natural bones.



[114] However, the mismatch of mechanical strengths between metallic grafts and natural bones can lead to bone resorption and therapeutic failure.<sup>[26]</sup> With conventional methods, it is difficult to obtain metal scaffolds with personalized external shapes and complex internal architecture; thus, innovative methods to develop scaffolds with biomimetic structures and mechanical properties are needed. With the rapid development of 3D metal printing, it is now feasible to print metallic implants with controllable porosity and modulus that closely match native bones, thereby restoring bone function and promoting bone regeneration. Titanium, a bioinert material, has been widely used in bone tissue engineering due to its excellent immune toleration.<sup>[115]</sup> Significant efforts have been made to enhance the biocompatibility and osteoconductivity of titanium scaffolds.<sup>[116]</sup> For instance, Song et al. demonstrated a series of strategies to modify titanium scaffolds, including electrochemical deposition, heat treatment, and alkali treatment.<sup>[79, 116]</sup> Compared with titanium, tantalum has modulus and elasticity closer to bones, which can reduce the complications and failures caused by stress-shielding. To fabricate 3D printed tantalum scaffolds for bone regeneration, Wang and colleagues reported an SLS-based strategy. Compared with titanium scaffolds fabricated using the same method, researchers demonstrated that the 3D printed tantalum scaffolds had equivalent biological performances, showing promising applications for bone regeneration.<sup>[80]</sup> The topological structure of 3D printed porous scaffolds can be customized and precisely fabricated. Customized topological structure and mechanical property of the printed scaffolds could better mimic natural bones, enhancing the osteogenic activity, and accelerating bone regeneration.<sup>[117]</sup> In one example, Dong et al. reported a room temperature extrusion-based 3D printing strategy to fabricate topologically ordered porous Mg scaffolds as bone-substituting implants. Briefly, after a solvent-cast-based 3D printing procedure binder in the ink was removed by debinding and sintering. Then, liquid-phase sintering was performed to generate the Mg scaffolds with hierarchical and interconnected porous structures.<sup>[81]</sup> In another work, Li and co-workers presented a strategy to fabricate topologically ordered porous iron scaffolds by direct metal printing (DMP). Metal scaffolds equipped with interconnected porous structures, as well as bone-mimicking mechanical strength and biodegradability, were demonstrated. The topological design based on repetitive diamond unit cells promoted biodegradation, making this strategy promising in 3D printing of biodegradable metal scaffolds.<sup>[82]</sup> In summary, porous 3D scaffolds with customized topology are promising in bone tissue engineering. However, requirements for high printing resolution and limitations of available materials need to be addressed.

Integrating ceramics, hydrogel-based materials, or other bioactive components in 3D-printed metal scaffolds is a common strategy to adjust the mechanical strength and promote the biocompatibility and osteogenesis of metallic scaffolds. To enhance the biocompatibility and osteoconductivity, Yang et al. introduced a 3D printing technique with HA coating to modify the macropores and surface structures of 3D printed iron scaffolds. The HA-coated and 3D printed iron scaffolds with natural bone strength were shown to promote *in vitro* viability and osteogenic differentiation of BMSCs.<sup>[83]</sup> With the further integration of hydrogel, the researchers demonstrated that it is feasible to load cells in 3D printed metal scaffolds. After infiltrating osteoblast-loaded bioactive hydrogel comprising of alginate, gelatin, and HA, Kumar et al. built a composited 3D printed Ti-6Al-4V scaffold promising for bone regeneration.<sup>[84]</sup>

Nanodiamonds have also been employed for modifying surfaces of bone implants.<sup>[118]</sup> With biological inertness and functional groups around the diamond core, such as -COOH, -NH<sub>2</sub>, and -OH, nanodiamond-interfaced 3D printed scaffolds can stimulate the proliferation and differentiation of cells.<sup>[119]</sup> For instance, Rifai and colleagues fabricated a 3D printed scaffold with nanodiamond (ND) coating. The coated nanodiamonds facilitated cell ingrowth and inhibited colonization of *Staphylococcus aureus*, paving a way to create antifouling 3D printed titanium scaffolds for biomedical implants.<sup>[85]</sup> Platelet-rich plasma-based scaffolds have been demonstrated to accelerate bone regeneration in clinical trials.<sup>[120]</sup> To enhance the biological performance of 3D printed titanium scaffold, researchers fabricated a composited 3D printed titanium scaffold with autologous platelet-rich plasma that could promote the ingrowth and osteogenic differentiation of BMSCs.<sup>[86]</sup> In summary, surface modifications with ceramics, hydrogel-based materials, or other bioactive components can endow 3D printed metallic scaffolds with better biocompatibility and osteogenic performance.

### 2.3 Hybrid scaffolds

Bones are composites comprising both inorganic and organic components that are organized in complex architectures serving distinct functions.<sup>[121]</sup> Therefore, hybrid scaffolds/ constructs fabricated from materials with different features could contribute to advanced bone tissue engineering. To further mimic the bone composition, various inorganic materials have been incorporated to the organic scaffolds given their chemical and mechanical similarity to natural bone minerals. For example, synthetic HA, which is similar to the main component of calcium phosphate minerals within bones and teeth, has been widely used in bone substitutes or implants to enhance mechanical strength and osteoconductivity. By using HA, carboxymethyl chitosan (CMCS), and polydopamine (PDA), Chen et al. printed degradable HA/CMCS/PDA scaffolds for fixing femoral condyle defects. They demonstrated that the printed HA/CMCS/PDA scaffolds could effectively promote new bone formation without causing inflammation in the implanted region. Moreover, the printed HA/CMCS/PDA scaffolds displayed biodegradability that matched the formation of new bones.<sup>[87]</sup> In another example, Yang and co-workers reported a 3D printing strategy using a cross-linkable nanocomposite ink consisted of hydroxyethyl methacrylate (HEMA)-functionalized HA nanoparticles (nHAMA) and tri-block poly (lactide-co-propylene glycol-co-lactide) dimethacrylate (PmLnDMA). The researchers found that an inorganic-organic co-crosslinked nanocomposite network with improved mechanical performances could be formed by crosslinking PmLnDMA and nHAMA, followed by adding inorganic components. The bone grafts printed using this nanocomposite ink showed enhanced osteoconductivity both *in vitro* and *in vivo* (Figure 3).<sup>[88]</sup>

In addition to HA, decellularized bone and other bioactive ceramics, such as  $\beta$ -tricalcium phosphate ( $\beta$ -TCP) and bioactive glass, have been investigated to optimize the mechanical property and osteogenic capability of printed scaffolds. As one of the most commonly used calcium phosphate ceramics,  $\beta$ -TCP has excellent osteoconductivity and biocompatibility. In comparison to HA,  $\beta$ -TCP has a faster degradation rate that can benefit the formation of new bones.<sup>[5, 122]</sup> In addition, magnesium (Mg), one of the most important components of natural bone, can promote mineral calcification deposition<sup>[123, 124]</sup>, cell adhesion, proliferation, and

osteogenic differentiation<sup>[123, 125]</sup>. By using a novel ink comprising  $\beta$ -TCP, Mg powder, and poly(lactic-co-glycolic acid) (PLGA), Lai's group printed porous PLGA/TCP/Mg scaffolds to accelerate bone regeneration in steroid-associated osteonecrosis. The researchers found that the PLGA/TCP/Mg scaffolds significantly enhanced neo-bone formation, vessel ingrowth, and blood perfusion in rabbit steroid-associated osteonecrosis models. The enhanced therapeutic efficacy can be ascribed to the bio-mimic structure of scaffolds and the release of Mg ion.<sup>[89]</sup> Bioactive glass is a commonly used biodegradable material in bone tissue engineering. It induces the formation of HA-like surface layer after implantation or simulated body fluid (SBF) immersion, which can promote the binding of soft tissues with hard ones.<sup>[126]</sup> Du et al. blended SF and mesoporous bioactive glass (MBG) to 3D print a biodegradable scaffold with good mechanical properties. The MBG/SF scaffolds significantly enhanced the expression of osteogenic COL-1, BSP, OCN, and BMP-2 *in vitro*. After loading with hBMSCs, the MBG/SF scaffolds promoted heterotopic bone formation *in vivo*.<sup>[90]</sup> In the last decade, scaffolds with tissue-specific extracellular matrix (ECM) have drawn increased interest for bone tissue engineering. The incorporated tissue-specific ECM can regulate cell behaviors, enhancing the osteogenic activity of 3D printed scaffolds.<sup>[127]</sup> However, hyperacute rejection is a great challenge associated with ECM derived from allogeneic or xenogeneic bones. Targeting hyperacute rejection, an adverse effect of porcine tissue transplantation in primates caused by  $\alpha$ 1, 3-galactose, the authors used decellularized porcine bone (DCB) from  $\alpha$ 1, 3-galactosyltransferase-deficient pigs as the natural component of the scaffold. They observed that the incorporation of DCB significantly strengthened the scaffolds and promoted bone regeneration.<sup>[91]</sup>

Advanced biofabrication or printing strategies have also been demonstrated to further facilitate multimaterial printing and fulfil the advanced requirement in bone tissue engineering, such as printing non-planer bone shape, bone-tendon interface engineering, and vascularized bone engineering. Hinton et al. showed the printing of complex shapes *via* freeform reversible embedding of suspended hydrogels (named "FRESH").<sup>[92]</sup> Using thermoreversible gelatin as the support bath, complex non-planar geometry was printed within the bath. The authors demonstrated that a human femur bone CT imaging data could be processed into machine code and get printed with high fidelity using alignate. Bone tissues often interact with other tissue types that have dramatically different mechanical features. Using multichannel 3D plotting, Luo et al. printed biphasic organic-inorganic scaffolds with calcium phosphate cement (CPC) paste and alginate paste. The bipartite CPC-alginate/alginate scaffolds were engineered with different mechanical strengths and optimized for repairing osteochondral defects. The CPC-alginate portion of bipartite scaffolds could induce bone regeneration, and the portion with alginate only could promote cartilage regeneration.<sup>[93]</sup> The mild fabrication conditions allowed the loading of drugs and cells. In another work, the investigators used a similar process to printed biphasic organic-inorganic scaffolds. The scaffolds were made of CPC paste and cell-laden alginate-methylcellulose blend (alg/mc) bioink. By 3D plotting, tripartite scaffolds with cell-laden alg/mc layer, cell-laden CPC-alg/mc layer, and CPC layer, were engineered to promote the regeneration of articular cartilage, calcified cartilage, and subchondral bone, respectively.<sup>[94]</sup> Kokkinis et al. utilized a multimaterial direct-ink writing platform for fabricating polyurethane acrylate elastomer gradients with elastic modulus ranging three orders of

magnitude. The system is applicable for recreating complicated tendon-to-bone insertions and human intervertebral disc (IVD).<sup>[95]</sup> Engineering vascularized bone is another area that can be addressed by hybrid scaffolds fabrication. Zhang et al. demonstrated a vascularized bone regeneration strategy by 3D printing the scaffolds with hollow-pipe structures and bioactive ions *via* coaxial printing. The hollow pipes could promote the efficient infiltration of host blood vessels and the bioactive ions  $Mg^{2+}$ ,  $Ca^{2+}$ , and  $Si^{2+}$  could be released to facilitate angiogenesis.<sup>[96]</sup> Therefore, by integrating advances in materials engineering, various 3D printing innovations could be achieved for enhancing the treatment efficacy and fulfilling the unmet need in clinical settings.

### 3. 3D printed drug delivery systems for bone regeneration

Therapeutics, such as GFs, can control and regulate bioactivities of cells, and they have been widely employed in bone tissue engineering to promote osteogenesis.<sup>[128]</sup> By encapsulating therapeutics within a matrix or scaffold, they can be protected from degradation and locally delivered to defect regions, avoiding systemic delivery-associated adverse effects. With the development of 3D printing, it is now possible to fabricate personalized DDS with multiple components to achieve personalized drug delivery for enhanced therapeutic efficacy and reduced adverse effects. In this part, we summarize recent studies combining DDS and 3D printed scaffolds for enhanced bone tissue regeneration. This part has been structured by category of materials (Table 3).

#### 3.1 Organic systems

**3.1.1. Polymer-based systems**—3D-printed hydrogels with specific structures play an essential role in controlling spatial feature-dependent cell behaviors.<sup>[153]</sup> With different fabrication processes and chemical modifications, the mechanical properties of hydrogel can be adjusted accordingly. Mechanical flexibility is essential for 3D printing, and responsive delivery of biomolecules once implanted.<sup>[154]</sup> In addition, hydrogel is one of the most used drug delivery matrixes in bone tissue engineering. The tunable biodegradability and mechanical flexibility hydrogels can enable the controlled release of loaded cargos.<sup>[155]</sup> Additionally, with 3D printing, multiple biomolecules in promising to be precisely loaded with desired spatial distribution, enabled the programed drug release. For instance, researchers directly linked alginate with biomolecules such as bone formation peptide-1 (BFP-1) by EDC/NHS coupling reaction and printed alginate–BFP-1 hydrogel scaffolds with sustained delivery of therapeutic proteins for bone tissue engineering.<sup>[129]</sup>

However, it is still quite challenging to print large volumes of mechanically strong mono-component hydrogels. Solid materials, in this condition, can be combined with hydrogel for maintaining specific scaffold structures. PCL is an optimal printable alternative because of its biodegradability and low melting point.<sup>[156]</sup> Some previous studies have attempted to include dry collagen into 3D printed PCL–tricalcium phosphate scaffolds. The scaffolds could be simply dipped in the recombined human bone morphogenetic protein-2 (rhBMP-2) solution before application.<sup>[130]</sup> However, such dipping methods, despite being convenient, can result in inconsistent drug loading and unnecessary waste of rhBMP-2. For controllable drug loading and release, it is feasible to load drugs in a printable vehicle matrix. For

instance, Shim and co-workers proposed a mixture of PCL and PLGA as materials for scaffold production. rhBMP-2, encapsulated in the mixture of collagen and gelatin hydrogels, was printed into the PCL/PLGA scaffold through a multi-head deposition system. Controlled release (up to 28 days) of rhBMP-2 was observed. Faster bone healing was achieved in critical-sized rabbit bone defect models and it also avoided burst release-related inflammatory responses.<sup>[131]</sup>

In addition to hydrogel, organic polymers have been used as matrices or meshes to enhance the mechanical properties and further improve biological functions. Various 3D printing-based solid scaffolds approved by FDA or in clinical trials have shown remarkable efficacy for bone remodeling<sup>[157]</sup>, among which polylactic acid (PLA), PCL, PLGA, PEG are common compositions. In spite of desirable mechanical strength and tunable pore sizes, their general hydrophobicity limits cell compatibility and their ability for secondary functionalization.<sup>[9]</sup> In order to further improve the efficacy and reduce the healing time of bone repair, delivery of osteoinductive agents from such solid scaffolds is under extensive research, and protein-based therapeutics have shown great potential.<sup>[158]</sup> However, challenges remain with compatible loading of GFs within solid polymer matrices, maintenance of bioactivity during and after printing, and desired release profiles from the scaffolds for bone regeneration.

GF-based therapeutics have shown great efficacy in bone defect repair and bone tissue regeneration. In addition, the homogenous loading of these protein therapeutics directly within the scaffolds has the advantages of fewer fabrication steps, uniform loading, and accurate dosages. However, maintaining bioactivity during and after 3D fabrication remains challenging. Various strategies to address this are under investigation, including polymer modification, carrier protection, and alternative compatible fabrication methods.<sup>[21]</sup> For instance, Park et al. fabricated scaffolds with PLGA grafted hyaluronic acid (hyaluronic acid-PLGA) and BMP-2/PEG complexes by 3D printing. Thermal processing during printing can denature the encapsulated GFs. Using PEG, growth factors can be solubilized within the organic solvents, and a heated-air-blower/air-knife system can be used to rapidly evaporate the solvent while maintaining growth factor activities. The BMP-2 can be released from the porous scaffolds to enhance bone regeneration in calvarial bone defects of rats model (Figure 4).<sup>[132]</sup> Tarafder et al. fabricated an embedded system containing GF-loaded PLGA microspheres and PCL fibers. PLGA microsphere can help protect the encapsulated therapeutics during the fabrication process and extend their stability in the scaffold. Connective tissue growth factor (CTGF) and transforming growth-factor  $\beta$  (TGF- $\beta$ ) were loaded into such microspheres and showed enhanced healing efficacy in defected temporomandibular joint (TMJ) discs of the rabbit.<sup>[133]</sup>

Compared with thermal curing, UV curing of photopolymer is generally more compatible with loading GFs for scaffold fabrication and can avoid heat-induced denaturation of proteins. Lee. et al. used micro stereolithography to generate 3D poly (propylene fumarate) (PPF)/diethyl fumarate (DEF)-based scaffold incorporating BMP-2 loaded PLGA microspheres. PPF/DEF photopolymer can be 3D fabricated with high resolution and desired porous structure *via* UV curing, generating the mechanical properties beneficial for bone defect repair. Uniform suspension of BMP-2 loaded PLGA microspheres within

scaffolds allowed the release for up to 28 days, significantly enhancing the bone healing process.<sup>[134]</sup> Extrusion-based 3D manufacturing causes less disruption to the bioactivity of the GFs. Caetano et al. used composite ink PCL/graphene for extrusion-based additive fabrication, which allowed the direct loading of bioactive agents within the solid scaffolds. Graphene can not only enhance the mechanical strength of the scaffolds but also load P1-lateX protein for osteogenic differentiation.<sup>[135]</sup>

Another commonly used strategy in functionalizing solid scaffold is a surface coating, which can be compatible with more 3D fabrication methods.<sup>[159]</sup> Chen et al. developed a poly(dopamine) coating strategy for functionalizing 3D-printed polymer scaffolds to immobilize BMP-2 onto PLGA porous scaffolds. The biomimetic poly(dopamine) coating strategy prevented the denaturation of bioactive proteins during fabrication. Ponericin G1, an antimicrobial peptide, was added to prevent microbial infections.<sup>[136]</sup> Similarly, Kim et al. generated PCL/PLGA scaffolds that were subsequently modified with heparin-dopamine (Hep-DOPA). Heparin is capable of binding to various GFs for controlled release *via* electrostatic interactions, while dopamine was used to coat the surface of the scaffolds. By further coating the scaffold with BMP-2 sustained release of BMP-2 increased ALP activity and calcium deposition *in vitro*, enhancing bone regeneration *in vivo*.<sup>[137]</sup> However, compared with direct printing, it is difficult for customizing drug loading and programming drug release *via* surface coating.

**3.1.2 Bioprinting**—Hydrogels have been extensively used in 3D bioprinting for their biodegradability, biocompatibility, and tissue-mimicking properties. It's a promising strategy to load therapeutics by 3D printing. One commonly used hydrogel scaffold is alginate. When crosslinked with calcium ions, reversible bridges form within alginate, allowing the release of the encapsulated biomolecules.<sup>[160]</sup> However, for protein delivery, the problem of weak interaction between alginate and proteins needs to be solved.<sup>[161]</sup> To address this, Alblas et al. utilized gelatin microparticles (GMPs) in their alginate scaffolds. The researchers encapsulated BMP-2 into GMPs, dispersing them homogeneously in alginate that was later used for 3D bioprinting. It was reported that, compared with direct administration, alginate-mediated sustained release of BMP-2 promoted better bone formation. The researchers observed osteogenic differentiation and proliferation both *in vitro* and *in vivo* when employing their 3D fabricated alginate scaffolds.<sup>[138]</sup> To promote the interaction between alginate and protein for sustained protein delivery, chemical modification of alginate was also reported. Jisun and co-workers covalently modified alginate with sulfate. Structurally similar to heparin, alginate-sulfate showed an enhanced affinity with GFs known to contain a heparin-binding domain, such as BMP-2. In their research, the negatively charged sulfite ions showed electrostatic interactions with positively charged BMP-2. While preparing bioinks with various percentages of alginate and alginate-sulfate, the researchers identified the optimal ratio for loading osteoblasts and BMP-2. Compared with pure alginate, the mixed bioink-based scaffolds worked better in inducing bone tissue regeneration.<sup>[139]</sup> Similar to alginate, gelatin, and collagen, GelMA and methacrylated hyaluronic acid (MeHA) are regarded as applicable hydrogels for bone tissue printing, which can also be coupled with solid polymers. For instance, researchers employed BMP-2-loaded MeHA to bioprint the structure of a solid human lumbar vertebra. The

hyaluronic acid gels were modified with high rigidity, and the authors demonstrated that these biomimicking porous scaffold structures were promising in stimulating bone regeneration.<sup>[140]</sup>

### 3.2 Inorganic systems

In order to better recapitulate native structures, components, and mechanical properties of natural bones, 3D printed inorganic scaffolds have been extensively investigated. 3D printed scaffolds with a combined GF delivery system can compensate for the disadvantages of inorganic scaffolds and improve regeneration in bone defects. However, unlike organic candidates, elevated temperature and post-processing are always required during the 3D fabrication of inorganic scaffolds, making parallel printing of inorganic materials and drug delivery matrices a challenge. To address this issue, GF delivery matrices have been coated onto or infiltrated into the porous structure of inorganic scaffolds. Wang et al. printed a porous HA scaffold using micro-syringe extrusion, followed by a series of sintering procedures. Chitosan microspheres encapsulating BMP-2 were loaded onto the porous scaffolds through collagen coating. The developed system showed sustained release of BMP-2 and effectively promoted osteogenic differentiation and bone formation both *in vitro* and *in vivo* (Figure 5).<sup>[141]</sup> In another work, Li et al. fabricated a 3D-printed scaffold consisting of CaP cement and mesoporous silica. Drug loading was achieved by infiltrating the BMP-2 solution into the scaffold. Silica released from this system promoted the ingrowth of vascular tissue at the early stage, and the prolonged BMP-2 release significantly stimulated bone regeneration *in vitro* and *in vivo*.<sup>[142]</sup> To overcome the limitations of high-temperature sintering processes, such as unexpected crystallization, unstable shrinkage-induced cracking, and inactivation of loaded drugs, low-temperature fabrication of 3D printed ceramic systems has been investigated.<sup>[12]</sup> For example, Raja et al. reported a low-temperature strategy to fabricate calcium-deficient hydroxyapatite (CDHA) scaffolds using  $\alpha$ -TCP pastes and hydroxyl propyl methyl cellulose (HPMC). After printing, the dried scaffolds were subject to a hydrolysis reaction, transferring  $\alpha$ -TCP to CDHA in phosphate buffer saline (PBS) at 37 °C. The process takes place at physiological conditions, and therefore temperature-sensitive drugs can be loaded with  $\alpha$ -TCP pastes and printed in the personalized scaffolds.<sup>[143]</sup> In another work, Lode et al. reported a 3D plotting strategy to fabricate pasty calcium phosphate cement (P-CPC) scaffolds in a mild condition. After 3D plotting, the scaffolds were hardened in water for 4 days instead of sintering, making it applicable for temperature-sensitive drugs.<sup>[144]</sup>

Titanium and its alloys are widely used as hard tissue replacements due to their biocompatibility and minimal foreign body response.<sup>[6, 162]</sup> Incorporating therapeutics is a widely used strategy to enhance the biological performance of titanium scaffolds. Stok et al. 3D-printed a titanium scaffold with 120  $\mu$ m thick titanium struts and 240 to 730  $\mu$ m pores using the SLM technique. BMP-2 and fibroblast growth factor-2 (FGF-2) solubilized with gelatin were filled into the rat model with critical femoral bone defect.<sup>[145]</sup> Teng et al. fabricated a Ti<sub>6</sub>Al<sub>4</sub>V plate with pore size of 600  $\mu$ m. After micro-arc oxidation and CaP modification, BMP-2 was coated onto the surface of the scaffold. In a rabbit model of critical-sized parietal bone defect, sustained release of BMP-2 was observed with the ability to significantly promote bone regeneration.<sup>[146]</sup>

In summary, it is still a challenge to print metallic materials with a protein-loaded matrix due to the inactivation of drugs during the process. However, drug loading strategies *via* coating and infiltration are not suitable for a spatiotemporally specific release of drugs. To address this, the development of 3D printing techniques in mild conditions is needed.

### 3.3 Hybrid systems

Bone has a complex composite structure consisting of organic matrices (mostly type I collagen) and structured minerals (mostly CaP).<sup>[12]</sup> CaP ceramics resemble native teeth and bone bio-minerals, and they have good biodegradability, biocompatibility, and osteoconductivity.<sup>[163]</sup> To mimic the natural components of bone and enhance bone formation, CaP-based systems have been broadly applied in 3D-printed polymer-based scaffolds. Moreover, by engineering composited scaffolds with drug-loaded components *via* printing, bone regeneration can be further accelerated. For instance, Castro et al. set up a table-top SL printer and fabricated a 3D printed TGF- $\beta$ 1 delivery system for osteochondral regeneration. The composite ink was composed of PEG:PEGDA, nanocrystalline hydroxyapatite (nHA), and core-shell PLGA nanosphere loaded with TGF- $\beta$ 1. The nHA and prolonged TGF- $\beta$ 1 release from the microspheres promoted the proliferation and osteochondral differentiation of BMSCs.<sup>[147]</sup> Another work by Shim et al. reported that the 3D printed PCL/PLGA/ $\beta$ -TCP membrane scaffolds showed sustained release of rhBMP-2 to improve bone regeneration. Using a multi-head deposition system, PCL/PLGA/ $\beta$ -TCP mixtures were printed in a layer-by-layer manner, and the spaces between printed fibers were filled with collagen/rhBMP-2. This 3D printed BMP-2 delivery scaffold achieved sustained delivery of GF and excellent bone regeneration in a rabbit model with bilateral full-thickness calvarial defects.<sup>[148]</sup>

With multichannel printing/plotting strategy, biphasic inorganic-organic systems fabricated in mild conditions have also been applied in protein delivery. For instance, Ahlfeld et al. plotted biphasic scaffolds with CPC and alginate-gellan gum (AlgGG) pastes in a mild condition for loading a growth factor. After a layer-by-layer 3D plotting process, VEGF-laden scaffolds were incubated in CaCl<sub>2</sub> solution (1M, 10 min) for hydrogel crosslinking. The crosslinked scaffold was then incubated in a water-saturated atmosphere (37 °C, 3 days) for cement setting. The plotted scaffolds exhibited a desired VEGF release profile for bone regeneration.<sup>[149]</sup> The researchers further investigated the biological activities of VEGF-laden CPC-AlgGG scaffolds. The CPC-AlgGG scaffolds could induce the osteogenic differentiation of MSCs, and the released VEGF could stimulate endothelial cell proliferation. With implantation into the defected region of rat femur diaphysis, VEGF-laden CPC-AlgGG scaffolds could effectively promote bone regeneration.<sup>[150]</sup>

Since gold can be easily modified with proteins, there has been great interest in engineering gold for protein delivery.<sup>[164]</sup> Heo et al. utilized biodegradable thermoplastic PLA to produce reinforced microstructures by FDM. The woven microstructures enhanced the structural integrity of composite cell-laden hydrogels. Arginine-glycine-aspartate (RGD) peptide-conjugated gold nanoparticles were embedded within GelMA hydrogel and functioned as an osteoinductive agent by guiding adipose-derived stem cells (ADSCs) for bone remodeling.<sup>[151]</sup>



3D printing can also help to construct specific architectures for various processes that occur during bone regeneration. Vascularization, for instance, plays a central role in bone healing, and it can be stimulated with certain 3D fabricated structures.<sup>[165]</sup> Biomolecules in hydrogels with different concentrations and properties show various release rates, allowing sequential drug delivery. Aiming to release vascular endothelial growth factor (VEGF) prior to BMP-2 release, researchers loaded VEGF in 10% alginate/gelatin mixture while BMP-2 in 2% collagen. To induce DPSCs to form bones outside vessels, they printed VEGF at the center, setting up a hypoxic microenvironment for angiogenesis. Induced neovascularization emerged with precise spatial and temporal regulation.<sup>[152]</sup> Another work by Byambaa and colleagues used different methacryloyl substitutions to gelatin and obtained GelMA with different biodegradability to print scaffolds. The inner part, consisting of GelMA with a lower degree of methacryloyl modification, degrades more rapidly, allowing for the formation of channels that can participate in vessel remodeling. For the outer part of the scaffold, the authors incorporated osteogenic GelMA ink with VEGF as well as silicate nanoplatelets. By encapsulating cells in pre-gel with different concentrations of VEGF, researchers managed to bioprinting hydrogel cylinder rods into a pyramidal structure with gradient VEGF concentration to realize bone constructs with vasculature-mimicking structure (Figure 6).<sup>[64]</sup> In brief, 3D printing enables customization of multiple bone microstructures with specific cell and drug loadings. For future development, optimizations on 3D printing techniques and materials are still needed to improve the resolution.

#### 4. 4D printing systems for bone regeneration

3D printing has been widely applied to various biomedical fields, including bone tissue engineering. The integration of a ‘time’ dimension with 3D printing has been demonstrated as a new concept as ‘4D printing’. 4D printed modules are expected to change shape or functionalities over time or in response to external stimuli. The *in vivo* microenvironment and the regenerative process are dynamic in nature, so the desired functionality of printed scaffolds or DDS should better vary accordingly. Morrison et al. fabricated PCL-based scaffolds to treat infants with tracheobronchomalacia.<sup>[166]</sup> Their printed structures were initially customized as patient-specific scaffolds for patients under 1 year of age. Over the next three years, the scaffolds can adapt to the growth of the airways with both their shape and material composition changing over time. The authors referred to this property as “4D biomaterials”, showing that 4D printing has the potential to boost the development of next-generation scaffolds and DDS <sup>[23, 167]</sup>. Combined with the advantages of high spatial resolution of 3D printing, 4D printing could allow therapies to be used in both space- and time-dependent manners. Here, we summarized studies pertaining to the development of 4D printed systems that could be used in bone tissue regeneration.

Common features to pursue in 4D printing include change of scaffold morphology in response to external stimuli. Bone defects are generally irregular in shape, 4D printing can engineer shape-shifting scaffolds to fit irregular bone defects. Wang et al. reported a shape memory bone scaffold based on  $\beta$ -tricalcium phosphate/poly(lactic acid-co-trimethylene carbonate) (TCP/P(DLLA-TMC)), which was further modified with osteogenic peptide and black phosphorous nanosheets.<sup>[168]</sup> The black phosphorous nanosheets provided photothermal-responsive features, enabling the scaffolds to undergo shape reconfiguration.

The mechanical strength of the scaffolds was also changed after printing and NIR irradiation, making it more similar to native human cancellous bone. *In vivo* integration of such a scaffold to rat cranial bone defects improved new bone formation. Differential swelling of materials is another strategy commonly used to address changes in defect morphology. One early work by Gladman et al. developed a plant cell-inspired bioink composed of stiff cellulose fibrils and acrylamide matrices.<sup>[169]</sup> The printing process facilitated the unidirectional alignment of cellulose fibrils, leading to longitudinal elongation during the swelling process. Structures with complex curvatures could be filled and fitted after swelling of the materials. These approaches have also been used to generate curved trachea implants for cartilage regeneration. Kim et al. designed a photo-cross-linkable silk fibroin (Sil-MA) hydrogel to 4D print trachea mimetic implants. Digital light processing (DLP) was used as a biocompatible printing platform to crosslink the cell-embedded Sil-MA hydrogel in a layer-by-layer manner. By tuning the concentrations of Sil-MA and shapes of different layers, controllable swelling and the resulting shape morphing could be enabled. Different types of cells were further incorporated into separate layers of the hydrogel with mucosa cells in the base layer and chondrocytes in the patterned layer. After implantation into the host trachea *in vivo*, both epithelium and cartilage were formed at predicted locations.<sup>[170]</sup> Since most structures in nature are composed of materials with distinct properties, such as tendon-to-bone<sup>[171]</sup>, Kuang et al. demonstrated a 4D printed module with both variable stiffness and morphology-shifting capability (Figure 7).<sup>[172]</sup> The authors developed a curable ink with tunable mechanical properties dependent on the degrees of crosslinking, which could be controlled by adjusting the light intensity of greyscale light patterns. The design of light patterns allowed the printing of shape-customizable modules, and the authors demonstrated the printing of artificial limbs with soft muscles around stiff bone. Since the printed materials have tunable glass transition temperatures, processings of heating and cooling could generate a number of curved morphologies.

Apart from the features of tuning shape or mechanical strength, 4D printing could also achieve the on-demand release of bioactive molecules upon exposure to specific stimuli. In drug delivery, responsive DDSs are attracting an increasing interest due to their capability to control drug release profiles according to the surrounding environment or pathological stages.<sup>[173]</sup> Specific biological signals, abnormal pathological factors, and external stimuli can all be used for “smart” scaffold design.<sup>[174]</sup> Similarly, 4D printed drug delivery devices can integrate stimuli-dependent responses into the systems to control drug release.<sup>[175]</sup> Gupta et al. reported a 3D printed stimuli-responsive capsule with a core/shell structure that can achieve programmable release of drugs from hydrogel matrices (Figure 8).<sup>[176]</sup> The cores of the capsules were comprised of polyvinyl alcohol (PVA), ethylene glycol, and bioactive molecules, while the shells were composed of PLGA and plasmonic gold nanorods (AuNRs). AuNRs could selectively rupture the capsule when irradiated with a specific laser (determined by the size of AuNRs). Within the hydrogel matrices, these 3D printed capsules could be spatiotemporally “activated” for irradiation-dependent drug delivery.

## 5. Conclusion and perspective

3D-printed scaffolds have significantly progressed in tissue engineering, becoming a platform with customizable structural design and tunable mechanical properties. 3D printing

will play a significant role in the future of bone-graft implants with its ability to accurately control scaffold structure and composition at the microscale. It enables the production of personalized bone grafts. To enhance bone regeneration efficacy, current strategies in combining drug delivery matrices with tissue scaffolds require either a protein-protecting carrier or protein friendly printing techniques. It has been shown that enhanced bone regeneration efficacy can be observed both *in vitro* and *in vivo* when bioactive molecules are incorporated within 3D printed scaffolds with sustained or programmed release profiles. Moreover, by integrating cells within biological inks, it is possible to bioprint personalized implants with biomimic components and micro-structures to restore the structure and function of defected bone. These biomimic constructs with biological activities show great promise for clinical application in the future.

Challenges still exist in the development of these 3D printed implants in bone tissue engineering. Natural bone is composed of complex microstructures, and advances in 3D printing techniques and biomaterials are required to achieve higher printing resolution to promote their use in clinical settings. Previous studies have proven that mechanical loads can influence bone formation and the remodeling of defects.<sup>[177]</sup> Ideally, mechanical properties of implants should match the niche so that loads can be transmitted through the graft, avoiding secondary fractures.<sup>[178]</sup> Unfortunately, hydrogel-based materials are still far from meeting these requirements, even though various strategies have been developed to enhance their mechanical properties. Metal- and ceramic-based materials have strong mechanical properties; however, the elevated temperature is usually needed in post-processing of 3D printed parts. During sintering and solidification, the heterogeneous internal microstructures and non-uniform shrinkage may cause cracking, damaging the scaffolds. Moreover, the elevated temperature is not compatible with protein-based therapeutics. The bioactivity of proteins can be completely lost after the processing. Even though drug loading can be achieved by infiltration and coating, it remains challenging to precisely control drug dosage and release profiles with infiltration and coating-based methods. In this context, to achieve programmable drug loading and release, new direct printing strategies with optimized materials under mild fabrication conditions should be further explored. For bioprinting, there are still some challenges to overcome for facilitating clinical translation. For instance, higher resolutions and faster printing rates are needed to fabricate implants with anatomical sizes. In addition, the mechanical property of bioprinted constructs should match natural bone tissues. However, stabilization of hydrogel with higher polymer concentration or longer crosslinking time may have negative effects on injectability and cell viability. Moreover, the cells need to be easily available, easy to culture, and nonimmunogenic.

In general, demand for the application of 3D printing techniques in bone tissue engineering will surge in the coming years in light of their ability to customize medical devices in both defect-specific and patient-specific manners.<sup>[179]</sup> To meet these demands, process-property optimization and manufacturing cost control need to be further addressed to realize real-world clinical applications.

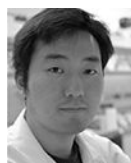
## Acknowledgement

M.Q., C.W., and X.Z. contributed equally to this work. This work has been supported by the National Institutes of Health fund to A.K. (AR057837, EB021857, AR073135).

## Biography



Moyuan Qu is a postdoctoral scholar in the Affiliated Stomatology Hospital, Zhejiang University School of Medicine. Before that, he was a visiting graduate researcher working with Prof. Ali Khademhosseini in the Center for Minimally Invasive Therapeutics at University of California-Los Angeles (UCLA). His research interests focus on scaffolds and drug delivery systems for regenerative medicine applications.



Wujin Sun is a Terasaki Fellow at the Terasaki Institute for Biomedical Innovation. He did his postdoctoral training at UCLA with Dr. Ali Khademhosseini. He completed his Ph.D. studies in the Joint Department of Biomedical Engineering at the University of North Carolina at Chapel Hill, and North Carolina State University. He is interested in integrating biomaterial engineering and cell engineering for healthcare applications.



Ali Khademhosseini is the Paul I. Terasaki Distinguished Professor and Director of the Terasaki Institute for Biomedical Innovation. From 2017 to 2020, he was the Levi Knight Professor of Bioengineering, Chemical Engineering and Radiology, and Founding Director of the Center for Minimally Invasive Therapeutics at UCLA. Before that, he was a professor of Medicine at Harvard Medical School. He is recognized as a leader in combining microengineering and nanoengineering approaches with advanced biomaterials for regenerative medicine applications.

In the past decade, development of multi-dimensional printing has significantly advanced the field of bone tissue engineering by fabricating scaffolds with biomimetic mechanical properties, architectures and programable drug release profiles. This review focuses on

summarizing recent advances in 3D printed scaffolds, 3D printed drug delivery systems (DDS) and 4D printing strategies for accelerated bone tissue regeneration.

## Reference

- [1]. Bose S, Vahabzadeh S, Bandyopadhyay A, *Materials today* 2013, 16, 496.
- [2]. Jones AC, Arns CH, Sheppard AP, Hutmacher DW, Milthorpe BK, Knackstedt MA, *Biomaterials* 2007, 28, 2491. [PubMed: 17335896]
- [3]. Seol Y-J, Kang T-Y, Cho D-W, *Soft Matter* 2012, 8, 1730.
- [4]. Khademhosseini A, Langer R, *Nature protocols* 2016, 11, 1775. [PubMed: 27583639]
- [5]. Stevens MM, *Materials today* 2008, 11, 18.
- [6]. Bose S, Roy M, Bandyopadhyay A, *Trends in biotechnology* 2012, 30, 546. [PubMed: 22939815]
- [7]. Suárez-González D, Lee JS, Diggs A, Lu Y, Nemke B, Markel M, Hollister SJ, Murphy WL, *Tissue Engineering Part A* 2013, 20, 2077; T. M. De Witte, L. E. Fratila-Apachitei, A. A. Zadpoor, N. A. Peppas, *Regen Biomater* 2018, 5, 197. [PubMed: 24350567]
- [8]. Liao CJ, Chen CF, Chen JH, Chiang SF, Lin YJ, Chang KY, *Journal of Biomedical Materials Research: An Official Journal of The Society for Biomaterials, The Japanese Society for Biomaterials, and The Australian Society for Biomaterials and the Korean Society for Biomaterials* 2002, 59, 676; A. Almirall, G. Larrecq, J. Delgado, S. Martinez, J. Planell, M. Ginebra, *Biomaterials* 2004, 25, 3671; H. Do Kim, E. H. Bae, I. C. Kwon, R. R. Pal, J. Do Nam, D. S. Lee, *Biomaterials* 2004, 25, 2319.
- [9]. Turnbull G, Clarke J, Picard F, Riches P, Jia L, Han F, Li B, Shu W, *Bioactive materials* 2018, 3, 278. [PubMed: 29744467]
- [10]. Hann SY, Cui H, Esworthy T, Miao S, Zhou X, Lee S.-j., Fisher JP, Zhang LG, *Translational Research* 2019, 211, 46. [PubMed: 31004563]
- [11]. Chia HN, Wu BM, *J Biol Eng* 2015, 9, 4. [PubMed: 25866560]
- [12]. Trombetta R, Inzana JA, Schwarz EM, Kates SL, Awad HA, *Annals of biomedical engineering* 2017, 45, 23. [PubMed: 27324800]
- [13]. Sawkins MJ, Mistry P, Brown BN, Shakesheff KM, Bonassar LJ, Yang J, *Biofabrication* 2015, 7, 035004; S. Adepu, N. Dhiman, A. Laha, C. S. Sharma, S. Ramakrishna, M. Khandelwal, *Current Opinion in Biomedical Engineering* 2017, 2, 22. [PubMed: 26133398]
- [14]. Sandler N, Preis M, *Trends Pharmacol Sci* 2016, 37, 1070. [PubMed: 27992318]
- [15]. Norman J, Madurawe RD, Moore CM, Khan MA, Khairuzzaman A, *Advanced drug delivery reviews* 2017, 108, 39. [PubMed: 27001902]
- [16]. Prasad LK, Smyth H, *Drug Dev Ind Pharm* 2016, 42, 1019. [PubMed: 26625986]
- [17]. Goyanes A, Chang H, Sedough D, Hatton GB, Wang J, Buanz A, Gaisford S, Basit AW, *International journal of pharmaceutics* 2015, 496, 414. [PubMed: 26481468]
- [18]. Carano RA, Filvaroff EH, *Drug discovery today* 2003, 8, 980. [PubMed: 14643161]
- [19]. Hernández A, Reyes R, Sánchez E, Rodríguez-Évora M, Delgado A, Évora C, *Journal of biomedical materials research Part A* 2012, 100, 2382. [PubMed: 22528545]
- [20]. Kempen DH, Lu L, Heijink A, Hefferan TE, Creemers LB, Maran A, Yaszemski MJ, Dhert WJ, *Biomaterials* 2009, 30, 2816; H. Wang, Q. Zou, O. C. Boerman, A. W. Nijhuis, J. A. Jansen, Y. Li, S. C. Leeuwenburgh, *Journal of Controlled Release* 2013, 166, 172; E. A. Bayer, J. Jordan, A. Roy, R. Gottardi, M. V. Fedorchak, P. N. Kumta, S. R. Little, *Tissue Engineering Part A* 2017, 23, 1382. [PubMed: 19232714]
- [21]. Park JY, Gao G, Jang J, Cho D-W, *Journal of Materials Chemistry B* 2016, 4, 7521. [PubMed: 32263809]
- [22]. Miao S, Castro N, Nowicki M, Xia L, Cui H, Zhou X, Zhu W, Lee S.-j., Sarkar K, Vozzi G, Tabata Y, Fisher J, Zhang LG, *Materials Today* 2017, 20, 577. [PubMed: 29403328]
- [23]. Gao B, Yang Q, Zhao X, Jin G, Ma Y, Xu F, *Trends in Biotechnology* 2016, 34, 746. [PubMed: 27056447]

- [24]. Kuang X, Chen K, Dunn CK, Wu J, Li VCF, Qi HJ, ACS Applied Materials & Interfaces 2018, 10, 7381; Q. Ge, A. H. Sakhaei, H. Lee, C. K. Dunn, N. X. Fang, M. L. Dunn, Scientific Reports 2016, 6, 31110. [PubMed: 29400445]
- [25]. Do AV, Khorsand B, Geary SM, Salem AK, Adv Healthc Mater 2015, 4, 1742. [PubMed: 26097108]
- [26]. Ni J, Ling H, Zhang S, Wang Z, Peng Z, Benyshek C, Zan R, Miri AK, Li Z, Zhang X, Lee J, Lee KJ, Kim HJ, Tebon P, Hoffman T, Dokmeci MR, Ashammakhi N, Li X, Khademhosseini A, Mater Today Bio 2019, 3, 100024.
- [27]. Zhang L, Yang G, Johnson BN, Jia X, Acta Biomater 2019, 84, 16; T. D. Ngo, A. Kashani, G. Imbalzano, K. T. Nguyen, D. Hui, Composites Part B: Engineering 2018, 143, 172. [PubMed: 30481607]
- [28]. Yilgor P, Sousa RA, Reis RL, Hasirci N, Hasirci V, “3D plotted PCL scaffolds for stem cell based bone tissue engineering”, presented at Macromolecular symposia, 2008; S. W. Kang, J. H. Bae, S. A. Park, W. D. Kim, M. S. Park, Y. J. Ko, H. S. Jang, J. H. Park, Biotechnol Lett 2012, 34, 1375.
- [29]. Park SA, Lee SH, Kim WD, Bioprocess Biosyst Eng 2011, 34, 505. [PubMed: 21170553]
- [30]. Akkineni AR, Luo Y, Schumacher M, Nies B, Lode A, Gelinsky M, Acta Biomater 2015, 27, 264. [PubMed: 26318366]
- [31]. Luo Y, Lode A, Gelinsky M, Adv Healthc Mater 2013, 2, 777. [PubMed: 23184455]
- [32]. Luo Y, Lode A, Wu C, Chang J, Gelinsky M, ACS Appl Mater Interfaces 2015, 7, 6541. [PubMed: 25761464]
- [33]. Kim G, Ahn S, Yoon H, Kim Y, Chun W, Journal of Materials Chemistry 2009, 19, 8817.
- [34]. Zhu H, Zhai D, Lin C, Zhang Y, Huan Z, Chang J, Wu C, J Mater Chem B 2016, 4, 6200. [PubMed: 32263632]
- [35]. Liu IH, Chang SH, Lin HY, Biomed Mater 2015, 10, 035004. [PubMed: 25970802]
- [36]. Luo Y, Wu C, Lode A, Gelinsky M, Biofabrication 2013, 5, 015005. [PubMed: 23228963]
- [37]. Guillaume O, Geven MA, Sprecher CM, Stadelmann VA, Grijpma DW, Tang TT, Qin L, Lai Y, Alini M, de Bruijn JD, Yuan H, Richards RG, Eglin D, Acta Biomater 2017, 54, 386. [PubMed: 28286037]
- [38]. Lee KW, Wang S, Fox BC, Ritman EL, Yaszemski MJ, Lu L, Biomacromolecules 2007, 8, 1077. [PubMed: 17326677]
- [39]. Arcaute K, Mann BK, Wicker RB, Ann Biomed Eng 2006, 34, 1429. [PubMed: 16897421]
- [40]. Le Guehennec L, Van Hede D, Plougonven E, Nolens G, Verlee B, De Pauw MC, Lambert F, J Biomed Mater Res A 2020, 108, 412. [PubMed: 31654476]
- [41]. Kang J-H, Jang K-J, Sakthiarami K, Oh G-J, Jang J-G, Park C, Lim H-P, Yun K-D, Park S-W, Ceramics International 2020, 46, 2481.
- [42]. Williams JM, Adewunmi A, Schek RM, Flanagan CL, Krebsbach PH, Feinberg SE, Hollister SJ, Das S, Biomaterials 2005, 26, 4817. [PubMed: 15763261]
- [43]. Duan B, Wang M, Zhou WY, Cheung WL, Li ZY, Lu WW, Acta Biomater 2010, 6, 4495; B. Duan, W. L. Cheung, M. Wang, Biofabrication 2011, 3, 015001. [PubMed: 20601244]
- [44]. Eshraghi S, Das S, Acta Biomater 2012, 8, 3138. [PubMed: 22522129]
- [45]. Kolan KC, Leu MC, Hilmas GE, Brown RF, Velez M, Biofabrication 2011, 3, 025004. [PubMed: 21636879]
- [46]. Shuai C, Mao Z, Lu H, Nie Y, Hu H, Peng S, Biofabrication 2013, 5, 015014. [PubMed: 23385303]
- [47]. Attar H, Calin M, Zhang L, Scudino S, Eckert J, Materials Science and Engineering: A 2014, 593, 170.
- [48]. Manakari V, Parande G, Gupta M, Metals 2017, 7, 2.
- [49]. Leuders S, Thöne M, Riemer A, Niendorf T, Tröster T, Richard H. a., Maier H, International Journal of Fatigue 2013, 48, 300.
- [50]. Sahmani S, Khandan A, Esmaeili S, Saber-Samandari S, Nejad MG, Aghdam M, Ceramics International 2020, 46, 2447.

- [51]. Xu N, Ye X, Wei D, Zhong J, Chen Y, Xu G, He D, ACS Appl Mater Interfaces 2014, 6, 14952. [PubMed: 25133309]
- [52]. Chen G, Chen N, Wang Q, Composites Science and Technology 2019, 172, 17.
- [53]. Wurm MC, Most T, Bergauer B, Rietzel D, Neukam FW, Cifuentes SC, Wilmowsky CV, J Biol Eng 2017, 11, 29. [PubMed: 28919925]
- [54]. Esposito Corcione C, Gervaso F, Scalera F, Montagna F, Sannino A, Maffezzoli A, Journal of Applied Polymer Science 2017, 134.
- [55]. Castilho M, Moseke C, Ewald A, Gbureck U, Groll J, Pires I, Teßmar J, Vorndran E, Biofabrication 2014, 6, 015006. [PubMed: 24429776]
- [56]. Castilho M, Rodrigues J, Pires I, Gouveia B, Pereira M, Moseke C, Groll J, Ewald A, Vorndran E, Biofabrication 2015, 7, 015004. [PubMed: 25562119]
- [57]. Inzana JA, Olvera D, Fuller SM, Kelly JP, Graeve OA, Schwarz EM, Kates SL, Awad HA, Biomaterials 2014, 35, 4026. [PubMed: 24529628]
- [58]. Gao G, Yonezawa T, Hubbell K, Dai G, Cui X, Biotechnology journal 2015, 10, 1568. [PubMed: 25641582]
- [59]. Gao G, Schilling AF, Hubbell K, Yonezawa T, Truong D, Hong Y, Dai G, Cui X, Biotechnology letters 2015, 37, 2349. [PubMed: 26198849]
- [60]. Gao G, Yonezawa T, Hubbell K, Dai G, Cui X, Biotechnol J 2015, 10, 1568. [PubMed: 25641582]
- [61]. Hernandez-Gonzalez AC, Tellez-Jurado L, Rodriguez-Lorenzo LM, Carbohydr Polym 2020, 229, 115514. [PubMed: 31826429]
- [62]. Bendtsen ST, Quinnell SP, Wei M, J Biomed Mater Res A 2017, 105, 1457. [PubMed: 28187519]
- [63]. Ojansivu M, Rashad A, Ahlinder A, Massera J, Mishra A, Syverud K, Finne-Wistrand A, Miettinen S, Mustafa K, Biofabrication 2019, 11, 035010. [PubMed: 30754034]
- [64]. Byambaa B, Annabi N, Yue K, Trujillo-de Santiago G, Alvarez MM, Jia W, Kazemzadeh-Narbat M, Shin SR, Tamayol A, Khademhosseini A, Advanced Healthcare Materials 2017, 6, 1700015.
- [65]. Lee H, Yang GH, Kim M, Lee J, Huh J, Kim G, Mater Sci Eng C Mater Biol Appl 2018, 84, 140. [PubMed: 29519423]
- [66]. Park SA, Lee SJ, Seok JM, Lee JH, Kim WD, Kwon IK, Journal of Bionic Engineering 2018, 15, 435.
- [67]. Wibowo A, Vyas C, Cooper G, Qulub F, Suratman R, Mahyuddin AI, Dirgantara T, Bartolo P, Materials (Basel) 2020, 13.
- [68]. Iandolo D, Ravichandran A, Liu X, Wen F, Chan JKY, Berggren M, Teoh S-H, Simon DT, Advanced Healthcare Materials 2016, 5, 1505. [PubMed: 27111453]
- [69]. Guex AG, Puetzer JL, Armgarth A, Littmann E, Stavrinidou E, Giannelis EP, Malliaras GG, Stevens MM, Acta Biomaterialia 2017, 62, 91. [PubMed: 28865991]
- [70]. Spencer AR, Shirzaei Sani E, Soucy JR, Corbet CC, Primbetova A, Koppes RA, Annabi N, ACS Applied Materials & Interfaces 2019, 11, 30518. [PubMed: 31373791]
- [71]. Duarte Campos DF, Blaeser A, Buellesbach K, Sen KS, Xun W, Tillmann W, Fischer H, Advanced Healthcare Materials 2016, 5, 1336. [PubMed: 27072652]
- [72]. Ouyang L, Armstrong JPK, Lin Y, Wojciechowski JP, Lee-Reeves C, Hachim D, Zhou K, Burdick JA, Stevens MM, Science Advances 2020, 6, eabc5529. [PubMed: 32948593]
- [73]. Diaz-Gomez L, Elizondo ME, Koons GL, Diba M, Chim LK, Cosgriff-Hernandez E, Melchiorri AJ, Mikos AG, Bioprinting 2020, 18, e00076. [PubMed: 33693067]
- [74]. Zhang M, Lin R, Wang X, Xue J, Deng C, Feng C, Zhuang H, Ma J, Qin C, Wan L, Chang J, Wu C, Sci Adv 2020, 6, eaaz6725. [PubMed: 32219170]
- [75]. Zeng H, Pathak JL, Shi Y, Ran J, Liang L, Yan Q, Wu T, Fan Q, Li M, Bai Y, Biofabrication 2020, 12, 025032. [PubMed: 32084655]
- [76]. Dang W, Ma B, Li B, Huan Z, Ma N, Zhu H, Chang J, Xiao Y, Wu C, Biofabrication 2020, 12, 025005. [PubMed: 31756727]
- [77]. Pan S, Yin J, Yu L, Zhang C, Zhu Y, Gao Y, Chen Y, Adv Sci (Weinh) 2020, 7, 1901511. [PubMed: 31993282]

- [78]. Yang Q, Yin H, Xu T, Zhu D, Yin J, Chen Y, Yu X, Gao J, Zhang C, Chen Y, Gao Y, Small 2020, 16, e1906814. [PubMed: 32108432]
- [79]. Song P, Hu C, Pei X, Sun J, Sun H, Wu L, Jiang Q, Fan H, Yang B, Zhou C, Fan Y, Zhang X, J Mater Chem B 2019, 7, 2865. [PubMed: 32255089]
- [80]. Wang H, Su K, Su L, Liang P, Ji P, Wang C, Mater Sci Eng C Mater Biol Appl 2019, 104, 109908. [PubMed: 31499974]
- [81]. Dong J, Li Y, Lin P, Leeftang MA, van Asperen S, Yu K, Tumer N, Norder B, Zadpoor AA, Zhou J, Acta Biomater 2020, 114, 497. [PubMed: 32771594]
- [82]. Li Y, Jahr H, Lietaert K, Pavanram P, Yilmaz A, Fockaert LI, Leeftang MA, Pouran B, Gonzalez-Garcia Y, Weinans H, Mol JMC, Zhou J, Zadpoor AA, Acta Biomater 2018, 77, 380. [PubMed: 29981948]
- [83]. Yang C, Huan Z, Wang X, Wu C, Chang J, ACS Biomaterials Science & Engineering 2018, 4, 608. [PubMed: 33418749]
- [84]. Kumar A, Nune KC, Misra RDK, J Tissue Eng Regen Med 2018, 12, 1133. [PubMed: 29134773]
- [85]. Rifai A, Tran N, Reineck P, Elbourne A, Mayes E, Sarker A, Dekiwadia C, Ivanova EP, Crawford RJ, Ohshima T, Gibson BC, Greentree AD, Pirogova E, Fox K, ACS Appl Mater Interfaces 2019, 11, 24588. [PubMed: 31199619]
- [86]. Qiao S, Shen Q, Li Z, Wu D, Zhu Y, Lai H, Gu Y, Materials & Design 2020, 108825.
- [87]. Chen T, Zou Q, Du C, Wang C, Li Y, Fu B, Mater Sci Eng C Mater Biol Appl 2020, 116, 111148. [PubMed: 32806300]
- [88]. Yang Y, Zhang Q, Xu T, Zhang H, Zhang M, Lu L, Hao Y, Fuh JH, Zhao X, Biomaterials 2020, 120378. [PubMed: 32932140]
- [89]. Lai Y, Li Y, Cao H, Long J, Wang X, Li L, Li C, Jia Q, Teng B, Tang T, Peng J, Eglin D, Alini M, Grijpma DW, Richards G, Qin L, Biomaterials 2019, 197, 207. [PubMed: 30660996]
- [90]. Du X, Wei D, Huang L, Zhu M, Zhang Y, Zhu Y, Mater Sci Eng C Mater Biol Appl 2019, 103, 109731. [PubMed: 31349472]
- [91]. Pan Q, Gao C, Wang Y, Wang Y, Mao C, Wang Q, Economidou SN, Douroumis D, Wen F, Tan LP, Bio-Design and Manufacturing 2020, 1.
- [92]. Hinton TJ, Jallerat Q, Palchesko RN, Park JH, Grodzicki MS, Shue H-J, Ramadan MH, Hudson AR, Feinberg AW, Science Advances 2015, 1, e1500758. [PubMed: 26601312]
- [93]. Luo Y, Lode A, Sonntag F, Nies B, Gelinsky M, J Mater Chem B 2013, 1, 4088. [PubMed: 32260961]
- [94]. Ahlfeld T, Doberenz F, Kilian D, Vater C, Korn P, Lauer G, Lode A, Gelinsky M, Biofabrication 2018, 10, 045002. [PubMed: 30004388]
- [95]. Kokkinis D, Bouville F, Studart AR, Advanced Materials 2018, 30, 1705808.
- [96]. Zhang W, Feng C, Yang G, Li G, Ding X, Wang S, Dou Y, Zhang Z, Chang J, Wu C, Jiang X, Biomaterials 2017, 135, 85. [PubMed: 28499127]
- [97]. Wang Y, Cui H, Wu Z, Wu N, Wang Z, Chen X, Wei Y, Zhang P, PLoS One 2016, 11, e0154924. [PubMed: 27149625]
- [98]. Vasquez-Sancho F, Abdollahi A, Damjanovic D, Catalan G, Adv Mater 2018, 30; J. Chen, M. Yu, B. Guo, P. X. Ma, Z. Yin, J Colloid Interface Sci 2018, 514, 517.
- [99]. Zamora-Sequeira R, Ardao I, Starbird R, García-González CA, Carbohydr Polym 2018, 189, 304. [PubMed: 29580413]
- [100]. El-Sherbiny IM, Yacoub MH, Glob Cardiol Sci Pract 2013, 2013, 316; X. Bai, M. Gao, S. Syed, J. Zhuang, X. Xu, X.-Q. Zhang, Bioactive Materials 2018, 3, 401; A. Pacifici, L. Laino, M. Gargari, F. Guzzo, A. Velandia Luz, A. Polimeni, L. Pacifici, International journal of medical sciences 2018, 15, 492. [PubMed: 24689032]
- [101]. Li J, Mooney DJ, Nature reviews. Materials 2016, 1, 16071; X. Tong, S. Lee, L. Bararpour, F. Yang, Macromolecular bioscience 2015, 15, 1679.
- [102]. Ashammakhi N, Hasan A, Kaarela O, Byambaa B, Sheikhi A, Gaharwar AK, Khademhosseini A, Adv Healthc Mater 2019, 8, e1801048; G. D. Nicodemus, S. J. Bryant, Tissue Engineering Part B: Reviews 2008, 14, 149. [PubMed: 30734530]



- [103]. Hong S, Sycks D, Chan HF, Lin S, Lopez GP, Guilak F, Leong KW, Zhao X, *Advanced Materials* 2015, 27, 4035; S. E. Bakarich, M. i. h. Panhuis, S. Beirne, G. G. Wallace, G. M. Spinks, *Journal of Materials Chemistry B* 2013, 1, 4939. [PubMed: 26033288]
- [104]. Cui H, Yu Y, Li X, Sun Z, Ruan J, Wu Z, Qian J, Yin J, *Journal of Materials Chemistry B* 2019, 7, 7207. [PubMed: 31663588]
- [105]. Murphy SV, Atala A, *Nature biotechnology* 2014, 32, 773.
- [106]. Ashammakhi N, Hasan A, Kaarela O, Byambaa B, Sheikhi A, Gaharwar AK, Khademhosseini A, *Advanced healthcare materials* 2019, 8, 1801048; S. Midha, M. Dalela, D. Sybil, P. Patra, S. Mohanty, *Journal of tissue engineering and regenerative medicine* 2019, 13, 925.
- [107]. Suchanek W, Yoshimura M, *Journal of Materials Research* 1998, 13, 94.
- [108]. LeGeros RZ, *Clinical Orthopaedics and Related Research* 2002, 395, 81.
- [109]. Liu D-M, *Ceramics International* 1997, 23, 135.
- [110]. Karageorgiou V, Kaplan D, *Biomaterials* 2005, 26, 5474. [PubMed: 15860204]
- [111]. Szuplewska A, Kulpińska D, Dybko A, Jastrzębska AM, Wojciechowski T, Rozmysłowska A, Chudy M, Grabowska-Jadach I, Ziemkowska W, Brzózka Z, *Materials Science and Engineering: C* 2019, 98, 874. [PubMed: 30813093]
- [112]. Sung YC, Jin PR, Chu LA, Hsu FF, Wang MR, Chang CC, Chiou SJ, Qiu JT, Gao DY, Lin CC, Chen YS, Hsu YC, Wang J, Wang FN, Yu PL, Chiang AS, Wu AY, Ko JJ, Lai CP, Lu TT, Chen Y, *Nat Nanotechnol* 2019, 14, 1160. [PubMed: 31740794]
- [113]. Damoulis PD, Drakos DE, Gagari E, Kaplan DL, *Ann N Y Acad Sci* 2007, 1117, 367. [PubMed: 17656569]
- [114]. Tellisi N, Ashammakhi NA, Billi F, Kaarela O, *Journal of Craniofacial Surgery* 2018, 29, 2363.
- [115]. Alvarez K, Nakajima H, *Materials* 2009, 2, 790.
- [116]. Garot C, Bettega G, Picart C, *Advanced Functional Materials* 2020, 2006967. [PubMed: 33531885]
- [117]. Wang X, Xu S, Zhou S, Xu W, Leary M, Choong P, Qian M, Brandt M, Xie YM, *Biomaterials* 2016, 83, 127; A. H. Yusop, A. A. Bakir, N. A. Shaharom, M. R. Abdul Kadir, H. Hermawan, *Int J Biomater* 2012, 2012, 641430. [PubMed: 26773669]
- [118]. Wu X, Bruschi M, Waag T, Schweetberg S, Tian Y, Meinhardt T, Stigler R, Larsson K, Funk M, Steinmüller-Nethl D, *Journal of Materials Chemistry B* 2017, 5, 6629; F. Zhang, Q. Song, X. Huang, F. Li, K. Wang, Y. Tang, C. Hou, H. Shen, *ACS Applied Materials & Interfaces* 2016, 8, 1087. [PubMed: 32264425]
- [119]. Jiang J, Papoutsakis ET, *Advanced healthcare materials* 2013, 2, 25; M. A. Yassin, K. Mustafa, Z. Xing, Y. Sun, K. E. Fasmer, T. Waag, A. Krueger, D. Steinmüller-Nethl, A. Finne-Wistrand, K. N. Leknes, *Macromol Biosci* 2017, 17. [PubMed: 23184458]
- [120]. Khairy NM, Shendy EE, Askar NA, El-Rouby DH, *Int J Oral Maxillofac Surg* 2013, 42, 249. [PubMed: 23078753]
- [121]. Soundrapandian C, Sa B, Datta S, *AAPS PharmSciTech* 2009, 10, 1158. [PubMed: 19842042]
- [122]. Cao H, Kuboyama N, *Bone* 2010, 46, 386. [PubMed: 19800045]
- [123]. Castiglioni S, Cazzaniga A, Albisetti W, Maier JA, *Nutrients* 2013, 5, 3022. [PubMed: 23912329]
- [124]. Abdallah M-N, Eimar H, Bassett DC, Schnabel M, Ciobanu O, Nelea V, McKee MD, Cerruti M, Tamimi F, *Acta biomaterialia* 2016, 37, 174. [PubMed: 27060619]
- [125]. Yoshizawa S, Brown A, Barchowsky A, Sfeir C, *Acta biomaterialia* 2014, 10, 2834; Z. Wu, Z. Meng, Q. Wu, D. Zeng, Z. Guo, J. Yao, Y. Bian, Y. Gu, S. Cheng, L. Peng, *Journal of Tissue Engineering* 2020, 11, 2041731420967791. [PubMed: 24512978]
- [126]. Rahaman MN, Day DE, Bal BS, Fu Q, Jung SB, Bonewald LF, Tomsia AP, *Acta biomaterialia* 2011, 7, 2355; T. Kokubo, H. Takadama, *Biomaterials* 2006, 27, 2907. [PubMed: 21421084]
- [127]. Cheng CW, Solorio LD, Alsberg E, *Biotechnol Adv* 2014, 32, 462. [PubMed: 24417915]
- [128]. Lee K, Silva EA, Mooney DJ, *Journal of the Royal Society Interface* 2010, 8, 153; P. Tayalia, D. J. Mooney, *Advanced materials* 2009, 21, 3269.
- [129]. Heo EY, Ko NR, Bae MS, Lee SJ, Choi B-J, Kim JH, Kim HK, Park SA, Kwon IK, *Journal of Industrial and Engineering Chemistry* 2017, 45, 61.

- [130]. Sawyer AA, Song SJ, Susanto E, Chuan P, Lam CX, Woodruff MA, Hutmacher DW, Cool SM, *Biomaterials* 2009, 30, 2479. [PubMed: 19162318]
- [131]. Shim JH, Kim SE, Park JY, Kundu J, Kim SW, Kang SS, Cho DW, *Tissue Eng Part A* 2014, 20, 1980. [PubMed: 24517081]
- [132]. Park JK, Shim J-H, Kang KS, Yeom J, Jung HS, Kim JY, Lee KH, Kim T-H, Kim S-Y, Cho D-W, Hahn SK, *Advanced Functional Materials* 2011, 21, 2906.
- [133]. Tarafder S, Koch A, Jun Y, Chou C, Awadallah MR, Lee CH, *Biofabrication* 2016, 8, 025003. [PubMed: 27108484]
- [134]. Lee JW, Kang KS, Lee SH, Kim J-Y, Lee B-K, Cho D-W, *Biomaterials* 2011, 32, 744. [PubMed: 20933279]
- [135]. Caetano GF, Wang W, Chiang W-H, Cooper G, Diver C, Blaker JJ, Frade MA, Bártolo P, *3D Printing and Additive Manufacturing* 2018, 5, 127.
- [136]. Chen L, Shao L, Wang F, Huang Y, Gao F, *RSC Advances* 2019, 9, 10494.
- [137]. Kim T-H, Yun Y-P, Park Y-E, Lee S-H, Yong W, Kundu J, Jung JW, Shim J-H, Cho D-W, Kim SE, *Biomedical Materials* 2014, 9, 025008. [PubMed: 24518200]
- [138]. Poldervaart MT, Wang H, van der Stok J, Weinans H, Leeuwenburgh SCG, Öner FC, Dhert WJA, Alblas J, *PLOS ONE* 2013, 8, e72610. [PubMed: 23977328]
- [139]. Park J, Lee SJ, Lee H, Park SA, Lee JY, *Carbohydrate Polymers* 2018, 196, 217. [PubMed: 29891290]
- [140]. Poldervaart MT, Goversen B, de Ruijter M, Abbadessa A, Melchels FPW, Öner FC, Dhert WJA, Vermonden T, Alblas J, *PLOS ONE* 2017, 12, e0177628. [PubMed: 28586346]
- [141]. Wang H, Wu G, Zhang J, Zhou K, Yin B, Su X, Qiu G, Yang G, Zhang X, Zhou G, Wu Z, *Colloids Surf B Biointerfaces* 2016, 141, 491. [PubMed: 26896655]
- [142]. Li C, Jiang C, Deng Y, Li T, Li N, Peng M, Wang J, *Sci Rep* 2017, 7, 41331. [PubMed: 28128363]
- [143]. Raja N, Sung A, Park H, Yun H.-s., *Ceramics International* 2020.
- [144]. Lode A, Meissner K, Luo Y, Sonntag F, Glorius S, Nies B, Vater C, Despang F, Hanke T, Gelinsky M, *J Tissue Eng Regen Med* 2014, 8, 682. [PubMed: 22933381]
- [145]. van der Stok J, Wang H, Amin Yavari S, Siebelt M, Sandker M, Waarsing JH, Verhaar JA, Jahr H, Zadpoor AA, Leeuwenburgh SC, Weinans H, *Tissue Eng Part A* 2013, 19, 2605. [PubMed: 23822814]
- [146]. Teng FY, Tai IC, Ho ML, Wang JW, Weng LW, Wang YJ, Wang MW, Tseng CC, *Mater Sci Eng C Mater Biol Appl* 2019, 105, 109879. [PubMed: 31546456]
- [147]. Castro NJ, O'Brien J, Zhang LG, *Nanoscale* 2015, 7, 14010. [PubMed: 26234364]
- [148]. Shim JH, Yoon MC, Jeong CM, Jang J, Jeong SI, Cho DW, Huh JB, *Biomed Mater* 2014, 9, 065006. [PubMed: 25384105]
- [149]. Ahlfeld T, Akkineni AR, Forster Y, Kohler T, Knaack S, Gelinsky M, Lode A, *Ann Biomed Eng* 2017, 45, 224. [PubMed: 27384939]
- [150]. Ahlfeld T, Schuster FP, Forster Y, Quade M, Akkineni AR, Rentsch C, Rammelt S, Gelinsky M, Lode A, *Adv Healthc Mater* 2019, 8, e1801512. [PubMed: 30838778]
- [151]. Heo DN, Castro NJ, Lee S-J, Noh H, Zhu W, Zhang LG, *Nanoscale* 2017, 9, 5055. [PubMed: 28211933]
- [152]. Park JY, Shim J-H, Choi S-A, Jang J, Kim M, Lee SH, Cho D-W, *Journal of Materials Chemistry B* 2015, 3, 5415. [PubMed: 32262513]
- [153]. Huang Q, Zou Y, Arno MC, Chen S, Wang T, Gao J, Dove AP, Du J, *Chem Soc Rev* 2017, 46, 6255. [PubMed: 28816316]
- [154]. Kloxin AM, Kloxin CJ, Bowman CN, Anseth KS, *Advanced materials (Deerfield Beach, Fla.)* 2010, 22, 3484; P. T. Smith, A. Basu, A. Saha, A. Nelson, *Polymer* 2018, 152, 42.
- [155]. Tan H, Marra KG, *Materials* 2010, 3, 1746.
- [156]. Ma Y, Xie L, Yang B, Tian W, *Biotechnology and Bioengineering* 2019, 116, 452. [PubMed: 30475386]
- [157]. Marcellin-Little DJ, Harrysson OL, *Small Animal Total Joint Replacement* 2013, 223.

- [158]. Schuckert K-H, Jopp S, Teoh S-H, Tissue Engineering Part A 2008, 15, 493.
- [159]. Grafahrend D, Heffels K-H, Beer MV, Gasteier P, Möller M, Boehm G, Dalton PD, Groll J, Nature Materials 2011, 10, 67. [PubMed: 21151163]
- [160]. Tønnesen HH, Karlsten J, Drug Development and Industrial Pharmacy 2002, 28, 621; F. E. Freeman, D. J. Kelly, Scientific Reports 2017, 7, 17042. [PubMed: 12149954]
- [161]. Lee KY, Mooney DJ, Progress in polymer science 2012, 37, 106; Ø. Arlov, F. L. Aachmann, E. Feyzi, A. Sundan, G. Skjåk-Bræk, Biomacromolecules 2015, 16, 3417. [PubMed: 22125349]
- [162]. Dabrowski B, Swieszkowski W, Godlinski D, Kurzydowski KJ, Journal of Biomedical Materials Research Part B: Applied Biomaterials 2010, 95, 53.
- [163]. Garcia-Gareta E, Coathup MJ, Blunn GW, Bone 2015, 81, 112; H. Yuan, K. Kurashina, J. D. de Bruijn, Y. Li, K. De Groot, X. Zhang, Biomaterials 1999, 20, 1799; P. Habibovic, T. M. Sees, M. A. van den Doel, C. A. van Blitterswijk, K. de Groot, J Biomed Mater Res A 2006, 77, 747. [PubMed: 26163110]
- [164]. Wang P, Wang X, Wang L, Hou X, Liu W, Chen C, Science and technology of advanced materials 2015, 16, 034610. [PubMed: 27877797]
- [165]. Miller JS, Stevens KR, Yang MT, Baker BM, Nguyen D-HT, Cohen DM, Toro E, Chen AA, Galie PA, Yu X, Chaturvedi R, Bhatia SN, Chen CS, Nature Materials 2012, 11, 768; J. Filipowska, K. A. Tomaszewski, Ł. Nied wiedzki, J. A. Walocha, T. Nied wiedzki, Angiogenesis 2017, 20, 291. [PubMed: 22751181]
- [166]. Morrison RJ, Hollister SJ, Niedner MF, Mahani MG, Park AH, Mehta DK, Ohye RG, Green GE, Science Translational Medicine 2015, 7, 285ra64.
- [167]. Gao B, Yang Q, Zhao X, Jin G, Ma Y, Xu F, Trends Biotechnol 2016, 34, 746; Y. C. Li, Y. S. Zhang, A. Akpek, S. R. Shin, A. Khademhosseini, Biofabrication 2016, 9, 012001. [PubMed: 27056447]
- [168]. Wang C, Yue H, Liu J, Zhao Q, He Z, Li K, Lu B, Huang W, Wei Y, Tang Y, Wang M, Biofabrication 2020, 12, 045025. [PubMed: 32736373]
- [169]. Sydney Gladman A, Matsumoto EA, Nuzzo RG, Mahadevan L, Lewis JA, Nature Materials 2016, 15, 413. [PubMed: 26808461]
- [170]. Kim SH, Seo YB, Yeon YK, Lee YJ, Park HS, Sultan MT, Lee JM, Lee JS, Lee OJ, Hong H, Lee H, Ajitero O, Suh YJ, Song SH, Lee KH, Park CH, Biomaterials 2020, 260, 120281. [PubMed: 32858503]
- [171]. Rossetti L, Kuntz LA, Kunold E, Schock J, Müller KW, Grabmayr H, Stolberg-Stolberg J, Pfeiffer F, Sieber SA, Burgkart R, Bausch AR, Nature Materials 2017, 16, 664. [PubMed: 28250445]
- [172]. Kuang X, Wu J, Chen K, Zhao Z, Ding Z, Hu F, Fang D, Qi HJ, Science Advances 2019, 5, eaav5790. [PubMed: 31058222]
- [173]. Qu M, Jiang X, Zhou X, Wang C, Wu Q, Ren L, Zhu J, Zhu S, Tebon P, Sun W, Khademhosseini A, Adv Healthc Mater 2020, 9, e1901714. [PubMed: 32125786]
- [174]. Lu Y, Aimetti AA, Langer R, Gu Z, Nature Reviews Materials 2016, 2, 1; Y. Lu, W. Sun, Z. Gu, J Control Release 2014, 194, 1; W. Sun, Q. Hu, W. Ji, G. Wright, Z. Gu, Physiological reviews 2016, 97, 189.
- [175]. Larush L, Kaner I, Fluksman A, Tamsut A, Pawar AA, Lesnovski P, Benny O, Magdassi S, Journal of 3D printing in medicine 2017, 1, 219.
- [176]. Gupta MK, Meng F, Johnson BN, Kong YL, Tian L, Yeh YW, Masters N, Singamaneni S, McAlpine MC, Nano Lett 2015, 15, 5321. [PubMed: 26042472]
- [177]. Kodama Y, Umemura Y, Nagasawa S, Beamer WG, Donahue LR, Rosen CR, Baylink DJ, Farley JR, Calcif Tissue Int 2000, 66, 298. [PubMed: 10742449]
- [178]. Zhang J, He F, Zhang W, Zhang M, Yang H, Luo Z-P, Bone research 2015, 3, 14048. [PubMed: 26273532]
- [179]. Sun W, Lee J, Zhang S, Benyshek C, Dokmeci MR, Khademhosseini A, Advanced Science 2019, 6.

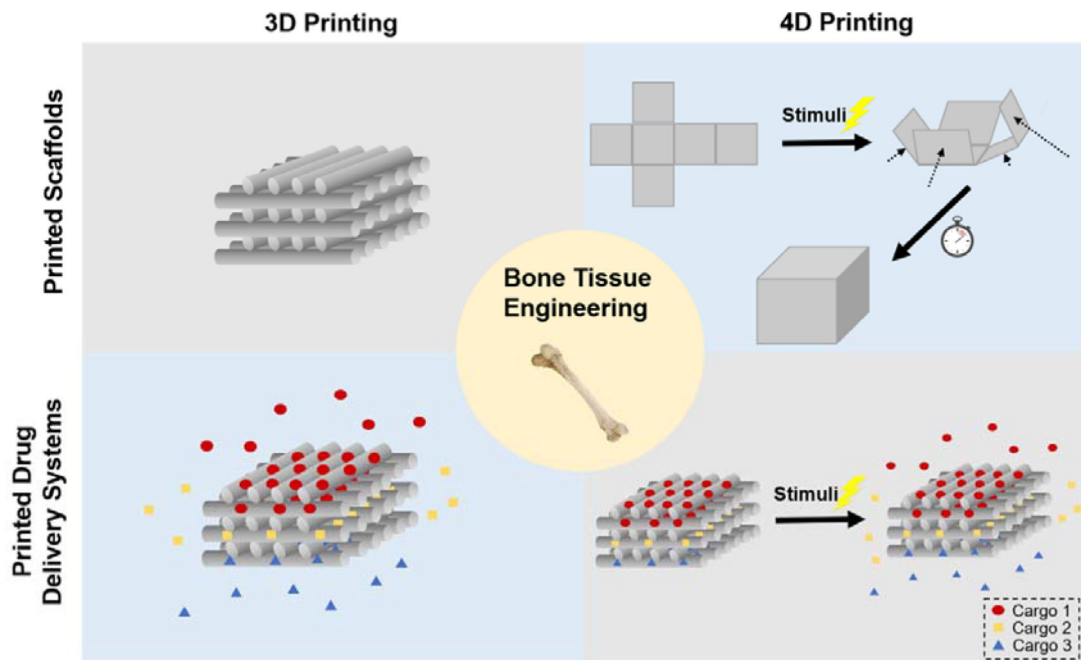


**Figure 1.** Schematic illustration of multi-dimensional printed scaffolds and DDS for bone tissue engineering. 3D printing techniques enable control of scaffold microstructures as well as composition. With 3D printing, it is possible to fabricate personalized DDS with multiple components and achieve personalized and programmed drug delivery. In addition to customized structures and compositions, 4D printed scaffolds and DDS are expected to sense signals within the physiological environment and change functionalities correspondingly, resulting in auto-adjusted structures or drug release profiles.

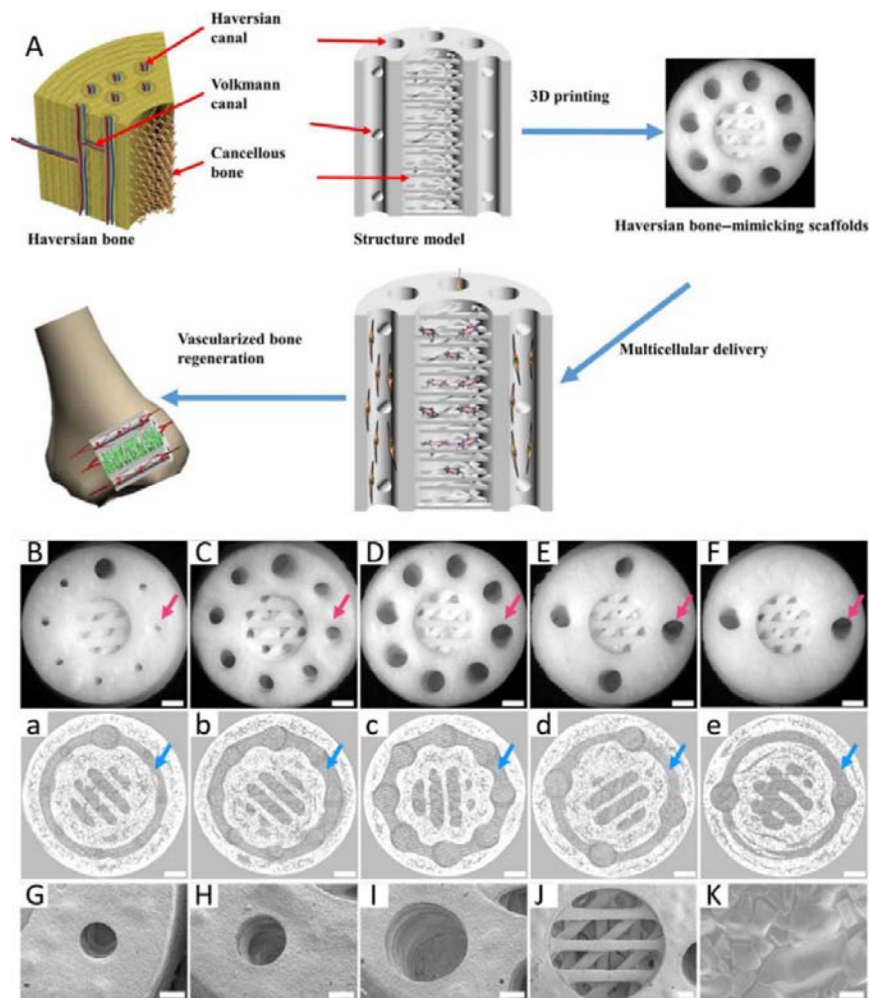
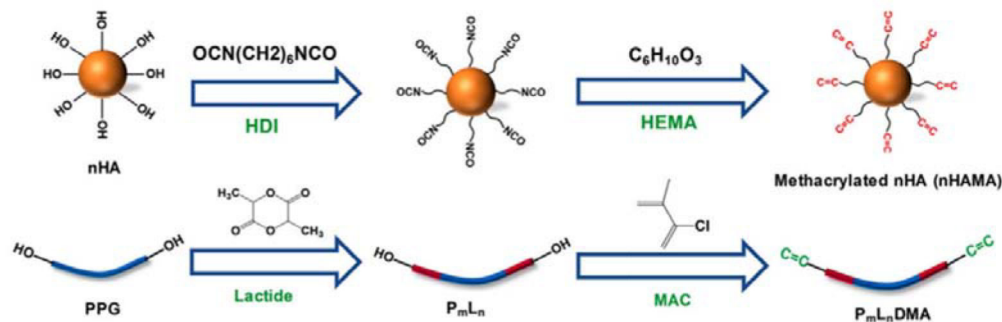


**Figure 2.** A. Schematic illustration and SEM images of 3D printed Haversian bone-mimicking scaffolds with  $\text{Ca}_2\text{MgSi}_2\text{O}_7$  bioceramic, 45S5 bioactive glass and photosensitive resin. These scaffolds were integrated with Haversian canals, Volkmann canals and cancellous bone structures. hBMSCs were seeded in cancellous bone mimic structures and HUVECs were seeded on Haversian canals. B-F. Optical microscope images of 3D printed Haversian bone-mimicking scaffolds with various diameters and numbers of Haversian canals (red arrows). Scale bars: 1 mm. a-e. Micro-CT images exhibited the connection between Volkmann canals (blue arrows) and Haversian canals in the interior of scaffolds. Scale bars, 1 mm. G-J. SEM images displayed the surface microstructure of the scaffolds. Scale bar: 400  $\mu\text{m}$ . K. Well-sintered surface of 3D printed Haversian bone-mimicking scaffolds. Scale bar: 6  $\mu\text{m}$ . Reproduced with permission.<sup>[74]</sup> Copyright 2020, AAAS.

**A. Material synthesis route**



**B. P<sub>m</sub>L<sub>n</sub>DMA-nHAMA co-crosslinked network**

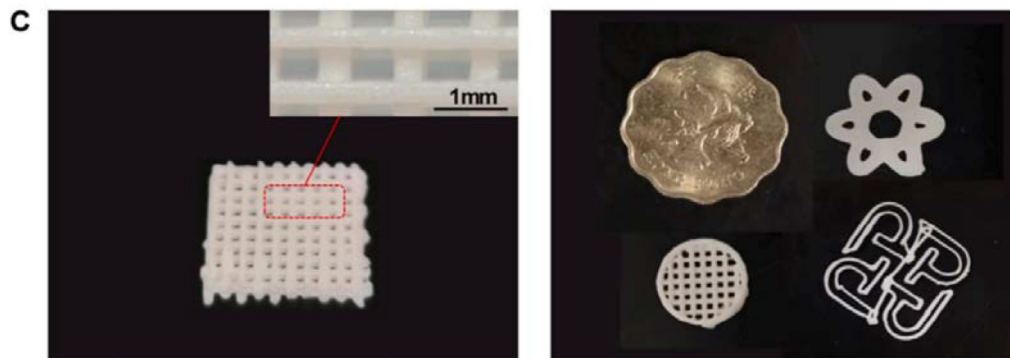
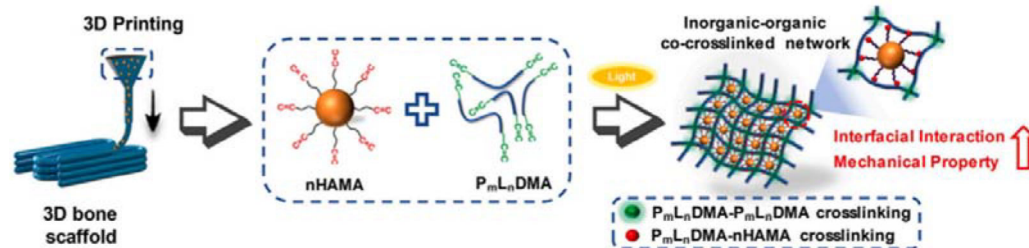


**Figure 3.** 3D printed scaffolds consisting of tri-block poly (lactide-co-propylene glycol-co-lactide) dimethacrylate (P<sub>m</sub>L<sub>n</sub>DMA) and hydroxyethyl methacrylate (HEMA)-functionalized hydroxyapatite nanoparticles (nHAMA). A. Schematic illustration of material synthesis. B. Schematic illustration of 3D printing process. The P<sub>m</sub>L<sub>n</sub>DMA-nHAMA co-crosslinked network improved the interfacial interaction and further enhanced the mechanical strength of scaffolds. C. Images of printed scaffolds with multiple 3D shapes printed with P<sub>7</sub>L<sub>2</sub>DMA/50% nHAMA composited ink. Reproduced with permission.<sup>[88]</sup> Copyright 2020, Elsevier.

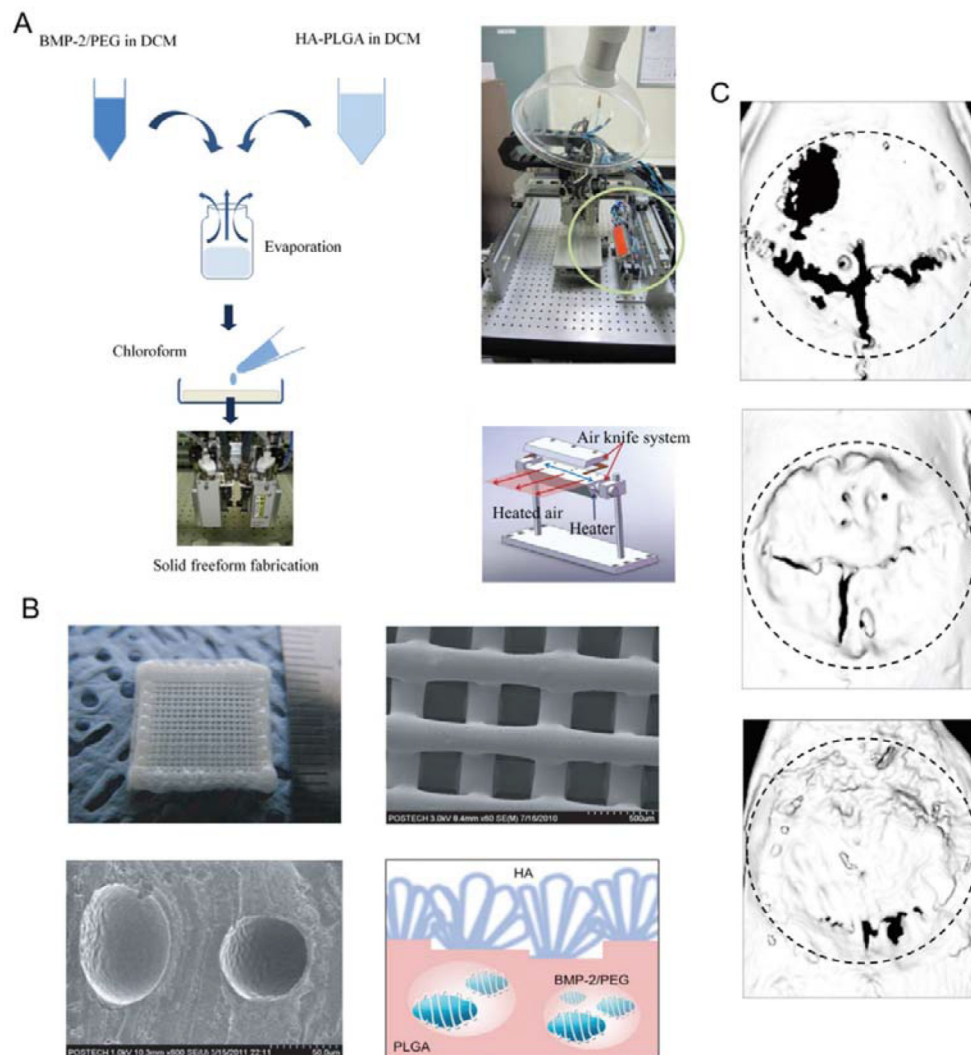


**Figure 4.** 3D printed tissue engineering scaffold with hyaluronic acid-PLGA encapsulating BMP-2/PEG complex. A. Schematic illustrations and photographs of the preparation of feeding solution and instruments for 3D printing of scaffolds using a multihead deposition system. B. Photographs and SEM images of 3D printed hyaluronic acid-PLGA/PEG/BMP-2 scaffold and BMP-2/PEG complexes within the fiber. C.  $\mu$ CT images of regenerated bones in calvarial bone defect model. (From top to bottom: control, hyaluronic acid-PLGA scaffold, and hyaluronic acid-PLGA/PEG/BMP-2 scaffold respectively). Reproduced with permission.<sup>[132]</sup> Copyright 2011, WILEY-VCH Verlag GmbH & Co. KGaA, Weinheim.

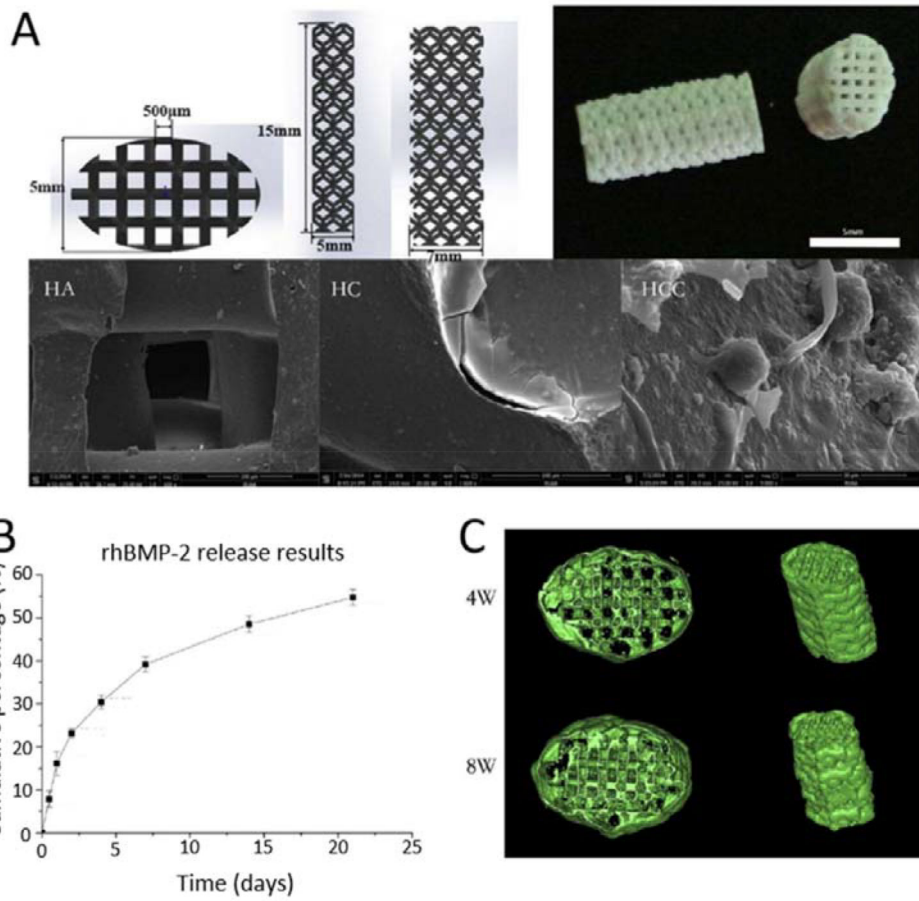


**Figure 5.** The 3D printed porous HA scaffold coated with BMP-2 loaded chitosan microspheres used for bone regeneration. A. Design, photograph and SEM images of 3D printed porous HA scaffold, collagen coated scaffold (HC) and collagen coated scaffold with BMP-2 loaded chitosan microspheres (HCC); B. *in vitro* release profile of BMP-2 from HCC; C.  $\mu$ CT images of ectopic bone formation with HCC after implantations for 4 week and 8 weeks. Reproduced with permission.<sup>[141]</sup> Copyright 2016, Elsevier.



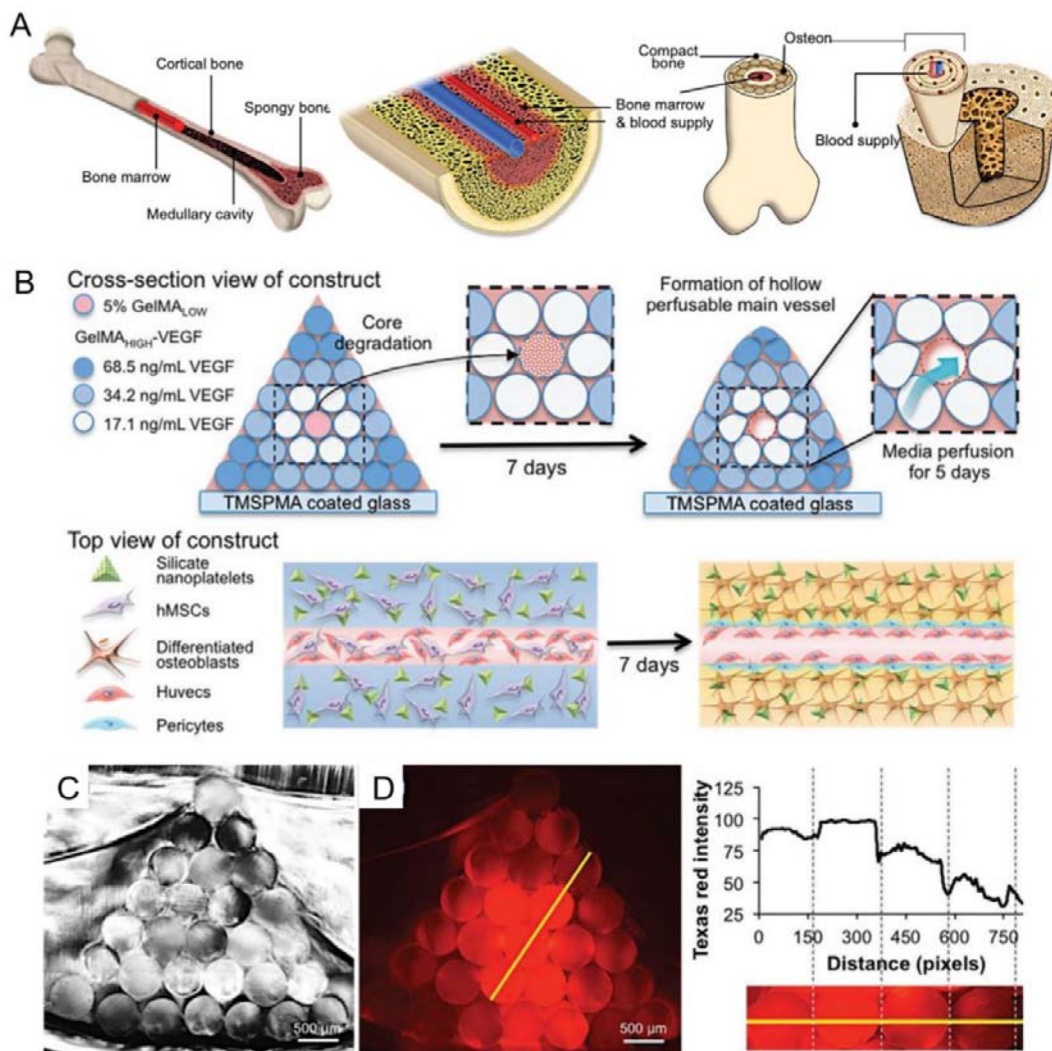


**Figure 6.** 3D bioprinting of bone mimetic 3D architecture with osteogenic and vasculogenic gradients. A. Schematic illustration of natural bone structure; B. Schematic illustration of 3D architecture with concentration gradients of VEGF. Central channel able to quickly degrade and favor the growth of HUVECs. C. Cross-section image of the printed hydrogel. D. Cross-section image of the printed gradual hydrogel with gradual concentrations of fluorochrome (Texas Red). Reproduced with permission.<sup>[64]</sup> Copyright 2017, WILEY-VCH Verlag GmbH & Co. KGaA, Weinheim.

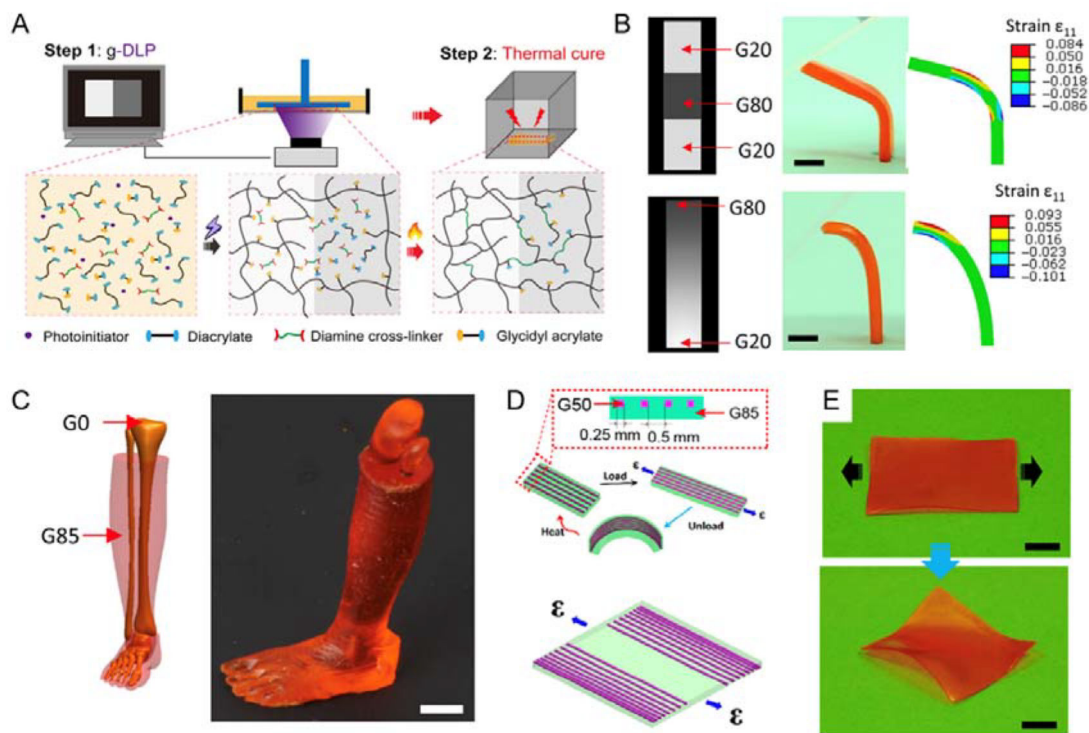


**Figure 7.**

A. Schematics of two-stage light and heating curing process of the g-DLP printing *via* graded material using hybrid ink. B. g-DLP printing *via* a discrete gradient and continuous gradient greyscale patterns and corresponding strain simulations. Scale bars, 5 mm. C. g-DLP printing of an artificial limb structure with stiff bone (G0) surrounded by soft muscle (G85). Scale bars, 1 cm. D. Design of a composite shape-shifting film by distributing fibers (G50) within the film (G85). E. Pictures of the printed shape-shifting film before and after the strain applications at room temperature. Scale bars, 1 cm. Reproduced with permission. [172] Copyright 2019, AAAS.

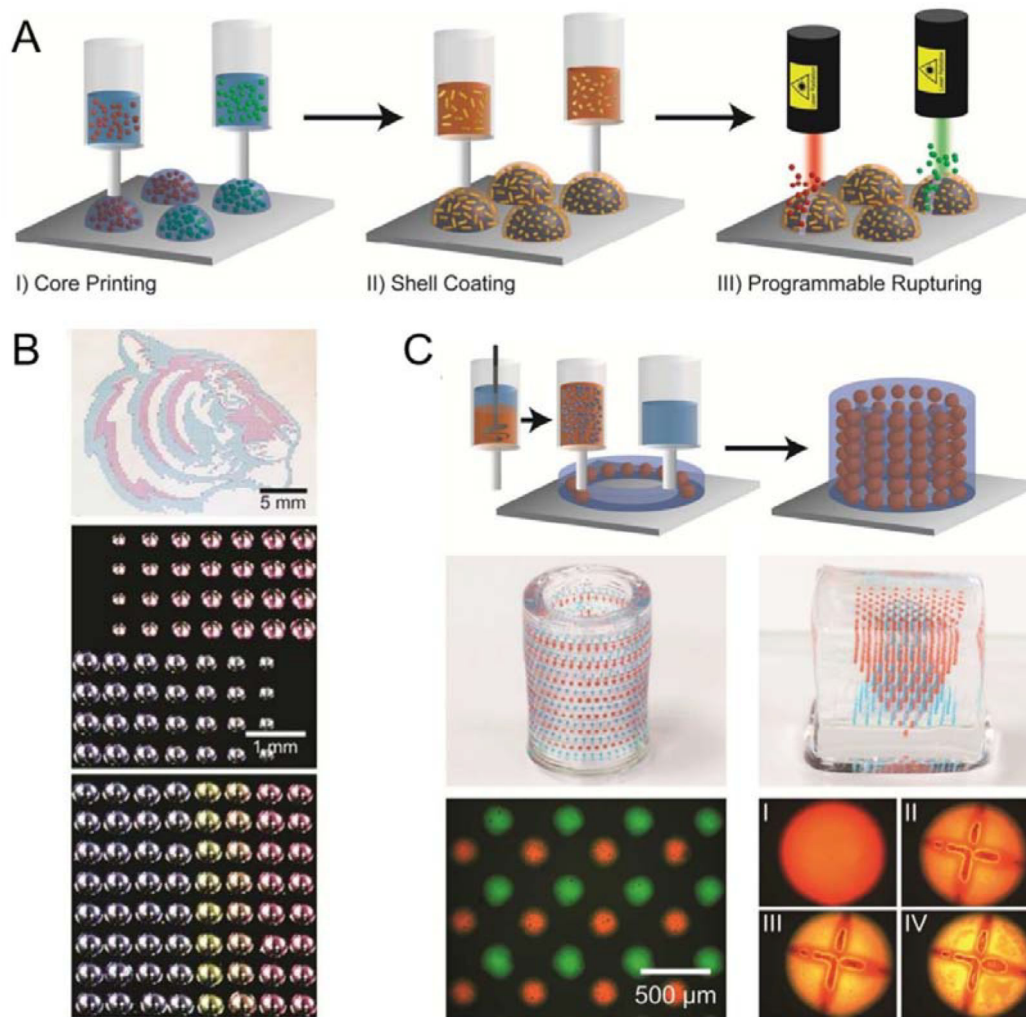


**Figure 8.** 3D printed responsive capsule with core/shell structures which can achieve programmable release of multiple drugs within a hydrogel matrix. A. Schematic illustration of the fabrication and rupturing of the responsive capsules, using laser. B. Optical micrographs of arrays with 3D printed capsules with different loading volume, distribution or multiple drug compositions; C. 3D printed hydrogel matrix with responsive capsules composed of multiple drugs allowing controlled capsule distributions. I-IV: Programed rupturing of the PLGA shell with plasmonic gold nanorods (AuNRs). (I: before laser rupture; II, III, IV: 15 min, 1 h, and 2 h after laser rupture) Reproduced with permission.<sup>[176]</sup> Copyright 2015, American Chemical Society.

**Table 1.**

3D printing techniques for bone implants fabrication.

3D printing techniques	Process	Materials	Advantages	Drawbacks
<b>3D plotting/direct ink writing</b>	The extrusion of injectable inks based on the predesigned shapes and structures	<ul style="list-style-type: none"> <li>● PCL<sup>[28]</sup></li> <li>● PCL/HA<sup>[29]</sup></li> <li>● CaP cement<sup>[30]</sup></li> <li>● Alginate<sup>[31]</sup></li> <li>● Alginate/Nano HA<sup>[32]</sup></li> <li>● Collagen<sup>[33]</sup></li> <li>● Bioceramic<sup>[34]</sup></li> <li>● Chitosan<sup>[35]</sup></li> <li>● Bioactive glass/alginate<sup>[36]</sup></li> </ul>	<ul style="list-style-type: none"> <li>● Mild conditions benefit the loading of biomolecules and cells</li> </ul>	<ul style="list-style-type: none"> <li>● A sintering process is needed for some materials</li> <li>● Low fabrication accuracy</li> </ul>
<b>Stereolithography (SLA)</b>	After exposure to focused light based on predesigned structure, polymer solidifies at focal points while polymer without exposure remains liquid.	<ul style="list-style-type: none"> <li>● PTMC/nano HA<sup>[37]</sup></li> <li>● PPF<sup>[38]</sup></li> <li>● PEG<sup>[39]</sup></li> <li>● HA/BCP/polyfunctional acrylic resins<sup>[40]</sup></li> <li>● Bioactive glass/rigid resin/1,6-hexanediol diacrylate<sup>[41]</sup></li> </ul>	<ul style="list-style-type: none"> <li>● Mild conditions benefit the loading of biomolecules and cells</li> <li>● High fabrication accuracy</li> <li>● Can obtain complex internal structures</li> </ul>	<ul style="list-style-type: none"> <li>● Photopolymer is needed</li> <li>● Defective biodegradation rates and biocompatibility</li> </ul>
<b>Selective laser sintering (SLS)</b>	A high-powered laser is used to sinter powder, thereby binding the material together to create a solid structure	<ul style="list-style-type: none"> <li>● PCL<sup>[42]</sup></li> <li>● CaP/PHBV<sup>[43]</sup></li> <li>● PCL/HA<sup>[44]</sup></li> <li>● Bioactive glass<sup>[45]</sup></li> <li>● PVA<sup>[46]</sup></li> </ul>	<ul style="list-style-type: none"> <li>● Needs no support structures</li> <li>● Fast</li> </ul>	<ul style="list-style-type: none"> <li>● Elevated temperatures</li> <li>● The resolution depends on the diameter of the laser beam</li> </ul>
<b>Selective laser melting (SLM)</b>	A high-powered laser is used to melt metal powder, then the scaffolds with the desired structure could be obtained after cooling	<ul style="list-style-type: none"> <li>● Pure titanium<sup>[47]</sup></li> <li>● Magnesium<sup>[48]</sup></li> <li>● TiAl<sub>6</sub>V<sub>4</sub><sup>[49]</sup></li> </ul>	<ul style="list-style-type: none"> <li>● Large range of metals available</li> </ul>	<ul style="list-style-type: none"> <li>● Elevated temperatures</li> <li>● The resolution depends on the diameter of the laser beam</li> </ul>
<b>Fused deposition modeling (FDM)</b>	The extrusion of heated polymer or ceramic with heated polymer binder and hardening post-printing to form a solid construct	<ul style="list-style-type: none"> <li>● CaP/PLA<sup>[50]</sup></li> <li>● PCL/HA<sup>[51]</sup></li> <li>● PVA/β-TCP<sup>[52]</sup></li> <li>● PLA<sup>[53]</sup></li> <li>● PLA/HA<sup>[54]</sup></li> </ul>	<ul style="list-style-type: none"> <li>● Needs no support structure</li> </ul>	<ul style="list-style-type: none"> <li>● Elevated temperatures</li> <li>● Low fabrication accuracy</li> </ul>
<b>Powder printing</b>	Jetting liquid binders onto powder bed to form each layer of desired construct. After fresh powders added, the process repeated layer by layer.	<ul style="list-style-type: none"> <li>● BCP/phosphoric acid<sup>[55]</sup></li> <li>● TCP/alginate/phosphoric acid<sup>[56]</sup></li> <li>● CaP/collagen/phosphoric acid<sup>[57]</sup></li> </ul>	<ul style="list-style-type: none"> <li>● Large range of materials available</li> </ul>	<ul style="list-style-type: none"> <li>● Low fabrication accuracy</li> <li>● Post-treatments (for example depowdering and sintering) are needed</li> </ul>
<b>Inkjet based bioprinting</b>	The ejection of bioinks from print head nozzle onto substrates with thermal or piezoelectric forces	<ul style="list-style-type: none"> <li>● PEGDMA<sup>[58]</sup></li> <li>● PEGDMA/GelMA<sup>[59]</sup></li> </ul>	<ul style="list-style-type: none"> <li>● Inexpensive</li> <li>● Compatible with low-viscosity biomaterials</li> </ul>	<ul style="list-style-type: none"> <li>● Low fabrication accuracy</li> <li>● Reduction of cell viability because of the eject force</li> </ul>
<b>Extrusion-based bioprinting</b>	After extruded under computer control, bioinks composed of cells and biomolecules were crosslinked to form desired structures	<ul style="list-style-type: none"> <li>● PEG<sup>[60]</sup></li> <li>● Alginate<sup>[61]</sup></li> <li>● Alginate/PVA/HA<sup>[62]</sup></li> <li>● Gelatin/Alginate<sup>[63]</sup></li> <li>● GelMA<sup>[64]</sup></li> </ul>	<ul style="list-style-type: none"> <li>● Mild conditions benefit the loading of biomolecules and cells</li> </ul>	<ul style="list-style-type: none"> <li>● Low mechanical properties</li> <li>● Low fabrication accuracy</li> <li>● Restriction of materials</li> </ul>

**PCL:** poly( $\epsilon$ -caprolactone), **HA:** hydroxyapatite, **CaP:** calcium phosphate, **PTMC:** Poly(trimethylene carbonate), **PPF:** Poly(propylene fumarate), **PEG:** polyethylene glycol, **BCP:** biphasic calcium phosphate, **PVA:** polyvinyl alcohol, **PLA:** polylactic acid,  **$\beta$ -TCP:**  $\beta$ -tricalcium phosphate, **PEGDMA:** poly(ethylene) glycol methacrylate, **GelMA:** gelatin methacrylate

**Table 2.**

Summary of 3D printed scaffolds for bone regeneration covered in this review.

Category	Sub-category	Materials	Biology evaluation	Reference
Organic scaffolds	Polymer-based scaffolds	Collagen/dECM/silk fibroin	<i>In vitro</i> : cell viability, proliferation and osteogenic activities of MC3T3-E1 cells	[65]
		PCL/PEG	<i>In vitro</i> : viability and osteogenic activities of MG63 cells	[66]
		PCL/PANI microparticles	<i>In vitro</i> : viability and proliferation of hADSCs	[67]
		PCL/PEDOT	<i>In vitro</i> : proliferation of MSCs	[68]
		PEDOT:PSS	<i>In vitro</i> : osteogenic activities of MC3T3-E1 cells	[69]
		PEDOT:PSS/GelMA	<i>In vitro</i> : viability of C2C12s cells <i>In vivo</i> : biodegradation and biocompatibility in rat	[70]
	Bioprinting	Agarose/collagen	<i>In vitro</i> : osteogenic differentiation of MSCs	[71]
		Gelatin/hyaluronic acid/chondroitin sulfate/dextran/alginate/chitosan/heparin/PEG	<i>In vitro</i> : osteogenic activity of osteogenic sarcoma cell line (Saos-2)	[72]
		PCL/GelMA/PLGA microparticles	<i>In vitro</i> : viability of fibroblasts	[73]
Inorganic scaffolds	Ceramics	Ca <sub>2</sub> MgSi <sub>2</sub> O <sub>7</sub> bioceramic/45S5 bioactive glass/photosensitive resin	<i>In vitro</i> : viability, proliferation, osteogenic differentiation of hBMSCs and angiogenic activities of HUVECs <i>In vivo</i> : bone and blood vessels regeneration in rabbit femoral defects	[74]
		BCP	<i>In vitro</i> : attachment, viability, proliferation and osteogenic and angiogenic activities of MC3T3-E1 cells; ERK1/2 inhibitor treatment analysis <i>In vivo</i> : regeneration of rabbit cranial bone defects	[75]
		metal-organic framework Cu-TCPP nanosheets/ $\beta$ -TCP	<i>In vitro</i> : anti-tumor efficacy with NIR light; cell attachments, osteogenic differentiation of hBMSCs and angiogenic activities of HUVECs <i>In vivo</i> : tumor ablation in nude mice; bone regeneration of rabbit femoral defects	[76]
		Mxene/bioactive glass	<i>In vitro</i> : cytotoxicity and cell ablation of Saos-2 cells with NIR light; proliferation and differentiation of hBMSCs <i>In vivo</i> : photothermal performance and tumor ablation in nude mice; bone regeneration of rat cranial defects	[77]
		mesoporous silica/Mxene/bioactive glass	<i>In vitro</i> : NO uptake and cell ablation of Saos-2 cells with NIR light; proliferation and differentiation of hBMSCs <i>In vivo</i> : photothermal performance and tumor ablation in nude mice; bone regeneration of rat cranial defects	[78]
	Metallic scaffolds	titanium	<i>In vitro</i> : attachment, viability, proliferation and osteogenic differentiation of BMSCs <i>In vivo</i> : the formation of new bone in rabbit femoral defects	[79]
		tantalum	<i>In vitro</i> : attachment, viability, proliferation and osteogenic differentiation of hBMSCs <i>In vivo</i> : bone formation in rabbit femoral defects	[80]
		magnesium	N.A.	[81]
		iron	<i>In vitro</i> : cell attachments and cytotoxicity of MG63 cells	[82]
		iron/HA	<i>In vitro</i> : viability and osteogenic differentiation of rabbit BMSCs	[83]
		titanium/alginate/nHA	<i>In vitro</i> : attachment, viability, proliferation and osteogenic activities of pre-osteoblasts	[84]
		titanium/nanodiamond	<i>In vitro</i> : attachment and proliferation of human fibroblasts and rat primary osteoblasts; anti-bacteria assay	[85]

Category	Sub-category	Materials	Biology evaluation	Reference
		titanium/autologous platelet -rich plasma	<i>In vitro</i> : viability and osteogenic differentiation of BMSCs <i>In vivo</i> : regeneration of femoral defects in rabbit osteoporosis models	[86]
Hybrid Scaffolds	N.A.	HA/carboxymethyl chitosan/polydopamine	<i>In vitro</i> : cytotoxicity and attachment of MC3T3-E1 cells <i>In vivo</i> : biosafety and regeneration of rabbit femoral condyle defects	[87]
		tri-block poly (lactide-co-propylene glycol-co-lactide) dimethacrylate and hydroxyethyl methacrylate functionalized HA nanoparticles	<i>In vitro</i> : cell viability, proliferation, and morphology of rMSCs <i>In vivo</i> : bone regeneration of rabbit femoral condyle defects	[88]
		PLGA/TCP/magnesium	<i>In vivo</i> : biosafety test and osteogenesis and angiogenesis in steroid associated osteonecrosis (SAON) rabbit model	[89]
		silk fibroin/bioactive glass	<i>In vitro</i> : cell attachment, viability, proliferation and osteogenic activities of hBMSCs <i>In vivo</i> : heterotopic bone formation	[90]
		PCL/decellularized porcine bone	<i>In vitro</i> : cell viability and osteogenic activities of hMSCs <i>In vivo</i> : bone regeneration of rat cranial bone defects	[91]
		Gelatin/Alginate/CaCl <sub>2</sub>	N.A.	[92]
		CPC/Alginate	<i>In vitro</i> : cell viability and osteogenic differentiation of MSCs	[93]
		CPC/alginate-methylcellulose blend	<i>In vitro</i> : cell viability of hTERT-MSC	[94]
		polyurethane acrylate elastomer	N.A.	[95]
		Ca <sub>7</sub> MgSi <sub>4</sub> O <sub>16</sub> bioceramic/sodium alginate/Pluronic F-127	<i>In vitro</i> : cell viability and osteogenic activities of BMSCs and angiogenic activities of HUVECs <i>In vivo</i> : bone regeneration of rabbit radius segmental defect model	[96]

**dECM**: decellularized extracellular matrix, **PCL**: poly( $\epsilon$ -caprolactone), **PEG**: polyethylene glycol, **PANI**: polyaniline, **PEDOT**: poly(3,4-ethylenedioxythiophene), **PEDOT:PSS**: poly(3,4-ethylenedioxythiophene):poly(styrenesulfonate), **PLGA**: poly(lactic-co-glycolic acid), **BCP**: biphasic calcium phosphate, **Cu-TCPP**: copper coordinated tetrakis (4-carboxyphenyl) porphyrin,  **$\beta$ -TCP**:  $\beta$ -tricalcium phosphate, **HA**: hydroxyapatite, **hADSCs**: human adipose-derived stem cells, **MSCs**: mesenchymal stem cells, **hBMSCs**: human bone mesenchymal stem cells, **HUVECs**: human umbilical vein endothelial cells, **CPC**: calcium phosphate cement, **hTERT-MSC**: human mesenchymal stem cell line expressing hTERT (human telomerase reverse transcriptase)

**Table 3.**

Summary of the 3D printed delivery systems for bone regeneration covered in this review

Category	Sub-category	Materials (Scaffold) <sup>1</sup>	Materials (Delivery matrix) <sup>2</sup>	Delivery matrix loading	Therapeutic	Evaluation	Reference
Organic Systems	Polymer-based systems	Alginate	Alginate	Chemical linkage	BFP-1	<i>In vitro</i> : hADSCs; NIH3T3; <i>In vivo</i> : calvarial bone defects of rabbits	[129]
		PCL-TCP	dry collagen	loading	Human recombinant BMP-2	<i>In vivo</i> : calvarial bone defects of rats	[130]
		PCL; PLGA	Collagen/gelatin	Printing	Human recombinant BMP-2	<i>In vivo</i> : rabbit radius segmental defect model	[131]
		HA-PLGA	PEG	Direct printing	BMP-2	<i>In vitro</i> : osteoblasts; <i>In vivo</i> : calvarial bone defects of SD rats	[132]
		PCL	PLGA microsphere	Direct printing	CTGF, TGF-β	<i>In vitro</i> : MSCs <i>In vivo</i> : temporomandibular joint disc in rabbits	[133]
		PPF/DEF	PLGA microspheres	Direct printing	BMP-2	<i>In vitro</i> : pre-osteoblasts <i>In vivo</i> : rat cranial bone defect	[134]
		PCL/graphene	graphene	Direct printing	P1-latex	<i>In vitro</i> : hADSCs	[135]
		PLGA	Poly (dopamine)	coating	BMP-2, Ponericin G1	<i>In vitro</i> : pre-osteoblasts	[136]
		PCL/PLGA	Heparin-dopamine	coating	BMP-2	<i>In vitro</i> : osteoblast-like cells (MG-63 cells) <i>In vivo</i> : rat femur bone defect	[137]
	Bioprinting	Alginate	Gelatin microparticles; Alginate	Encapsulation; printing	Human recombinant BMP-2	<i>In vitro</i> : goat multipotent stromal cells; <i>In vivo</i> : Subcutaneous implantation	[138]
		Alginate; Alginate-sulfate	Alginate; Alginate-sulfate	Direct printing	BMP-2	<i>In vitro</i> : MC3T3-E1 osteoblasts;	[139]
		MeHA	MeHA	Direct printing	BMP-2	N.A.	[140]
	Inorganic systems	CaP-based systems	HA	Chitosan microspheres	Coating	Human recombinant BMP-2	<i>In vitro</i> : hMSCs <i>In vivo</i> : ectopic bone formation model
calcium phosphate cement with mesoporous silica			N.A.	Infiltration	Human recombinant BMP-2	<i>In vitro</i> : HUVECs and hBMSCs <i>In vivo</i> : rabbit femoral defect model	[142]
CDHA			CDHA	Printing	Quercetin	N.A.	[143]
P-CPC			P-CPC	N.A.	N.A.	<i>In vitro</i> : hMSCs	[144]
Titanium-based systems		Titanium	Gelatin	Infiltration	BMP-2 and FGF-2	<i>In vivo</i> : critical femoral bone defects of rats	[145]
		CaP modified Ti <sub>6</sub> Al <sub>4</sub> V	N.A.	Coating	BMP-2	<i>In vivo</i> : calvarial bone defects of rabbits	[146]

Category	Sub-category	Materials (Scaffold) <sup>1</sup>	Materials (Delivery matrix) <sup>2</sup>	Delivery matrix loading	Therapeutic	Evaluation	Reference
Hybrid Systems	N.A.	PEG:PEGDA with nHA	PLGA	Printing	TGF-β1	<i>In vitro</i> : hMSC	[147]
		PCL/PLGA/β-TCP	Collagen	Printing	Human recombinant BMP-2	<i>In vivo</i> : rabbit calvarial defect model	[148]
		CPC	alginate-gellan gum	Printing	VEGF	<i>In vitro</i> : endothelial cell, HUVECs and MSCs <i>In vivo</i> : segmental bone defect in the rat femur	[149, 150]
		Polylactic acid	Gold NPs/ GelMA	Infiltration	BMP-2	<i>In vitro</i> : ADSCs	[151]
		PCL	Alginate; gelatin	Printing	VEGF	<i>In vitro</i> : DPSCs; <i>In vivo</i> : ectopic bone formation model	[152]
		PCL	Collagen	Printing	BMP-2		
		GelMA	GelMA	Printing	VEGF	<i>In vitro</i> : HUVECs and hMSCs	[64]

<sup>1</sup> materials for scaffold fabrications.

<sup>2</sup> materials of drug-loaded vehicles.

**PCL**: poly( $\epsilon$ -caprolactone), **TCP**: tricalcium phosphate, **PLGA**: poly(lactic-co-glycolic acid), **HA**: hydroxyapatite, **PEG**: polyethylene glycol, **PPF**: poly (propylene fumarate), **DEF**: diethyl fumarate, **MeHA**: methacrylated hyaluronic acid, **CaP**: calcium phosphate, **PEGDA**: polyethylene glycol diacrylate, **GelMA**: gelatin methacrylate, **BFP-1**: bone formation peptide-1, **BMP-2**: bone morphogenetic protein-2, **CTGF**: connective tissue growth factor, **TGF-β**: transforming growth factor-β, **FGF-2**: fibroblast growth factor-2, **VEGF**: vascular endothelial growth factor, **hADSCs**: human adipose-derived stem cell, **MSCs**: mesenchymal stem cells, **HUVECs**: human umbilical vein endothelial cells, **hBMSCs**: human bone mesenchymal stem cells, **DPSCs**: dental pulp stem cells, **CDHA**: calcium-deficient hydroxyapatite, **P-CPC**: pasty calcium phosphate cement, **CPC**: calcium phosphate cement